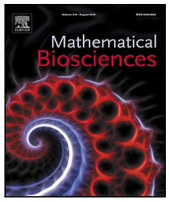
Mathematical Biosciences 377 (2024) 109302



Contents lists available at ScienceDirect

Mathematical Biosciences

journal homepage: www.elsevier.com/locate/mbs



Modeling virus-stimulated proliferation of CD4$^+$ T-cell, cell-to-cell transmission and viral loss in HIV infection dynamics

Jiawei Deng [a], Hongying Shu [a,*], Lin Wang [b], Xingfu Zou [c]

[a] School of Mathematics and Information Sciences, Guangzhou University, Guangzhou 510006, China
[b] Department of Mathematics and Statistics, University of New Brunswick, Fredericton, NB, E3B 5A3, Canada
[c] Department of Mathematics, University of Western Ontario, London, ON, N6A 5B7, Canada

ARTICLE INFO

Keywords:
Virus-stimulated proliferation
Cell-to-cell transmission
Global stability
Hopf bifurcation
Bistability

ABSTRACT

Human immunodeficiency virus (HIV) can persist in infected individuals despite prolonged antiretroviral therapy and it may spread through two modes: virus-to-cell and cell-to-cell transmissions. Understanding viral infection dynamics is pivotal for elucidating HIV pathogenesis. In this study, we incorporate the loss term of virions, and both virus-to-cell and cell-to-cell infection modes into a within-host HIV model, which also takes into consideration the proliferation of healthy target cells stimulated by free viruses. By constructing suitable Lyapunov function and applying geometric methods, we establish global stability results of the infection free equilibrium and the infection persistent equilibrium, respectively. Our findings highlight the crucial role of the basic reproduction number in the threshold dynamics. Moreover, we use the loss rate of virions as the bifurcation parameter to investigate stability switches of the positive equilibrium, local Hopf bifurcation, and its global continuation. Numerical simulations validate our theoretical results, revealing rich viral dynamics including backward bifurcation, saddle–node bifurcation, and bistability phenomenon in the sense that the infection free equilibrium and a limit cycle are both locally asymptotically stable. These insights contribute to a deeper understanding of HIV dynamics and inform the development of effective therapeutic strategies.

1. Introduction

As the pathogenic agent of the acquired immunodeficiency syndrome (AIDS), human immunodeficiency virus (HIV) has always been a considerable public health issue and widely spread around the world. More than 40 million people have lost their lives for HIV so far and there were an estimated 39 million people living with HIV at the end of 2022 [1]. It is well known that HIV invades the immune system and attacks the immune cells, such as CD4$^+$ T cells, which is the main driver of the immune response. To protect people from such sufferings, more and more scholars dedicate on the study of finding effective strategies for HIV prevention and treatment in their research fields [2–5].

In the past few decades, a great deal of mathematical models have been established to explore the effects of HIV on human immune system and characterize the mechanisms of HIV transmission [6–11]. In [6], a within-host infection model consisting of three compartments: uninfected target cells, infected cells and free viruses was introduced to explore the interaction between cells and viruses. A few more complex models were also constructed to figure out the biological process of HIV dissemination under therapy strategies. Immune system plays a crucial role in resisting viral invasion, Nowak and Bangham [7] established a standard within-host model considering the CTL immune response to examine the effects of individual variation in immune responsiveness on virus load and diversity. They discovered a nonintuitive result that strong and weak responders would be different in viral particles but many have similar levels of CTL response. On the basis of these classic models, time delays were incorporated into the biological models to examine the delay effects on viral dynamics [12]. The results suggested that time delays can induce Hopf bifurcation and sustained oscillations. Multiple HIV infection models were proposed to investigate the efficiencies of highly active antiretroviral therapy (HAART) on viral decay [13]. The conclusions showed that HIV cannot be eradicated and persist with a low level for many years under such treatment strategies. Great efforts have also been implemented to investigate the viral kinetics of other epidemics, such as HBV and HCV [14–16].

The classical HIV models [6,7] only consider the virus-to-cell transmission and healthy target cells are only infected by free viruses. However, an increasing number of works have revealed that another mode called cell-to-cell transmission also plays a significant role in HIV infection [2,3,17,18]. During this infection process, viral particles are transferred directly from an infected source cell to a susceptible

* Corresponding author.
E-mail address: hshu@snnu.edu.cn (H. Shu).

https://doi.org/10.1016/j.mbs.2024.109302

Available online 12 September 2024
0025-5564/© 2024 Elsevier Inc. All rights are reserved, including those for text and data mining, AI training, and similar technologies.

target cell through the formation of virological synapses [19]. By using mathematical analysis and calculation, Dixit and Perelson [20] discovered that genetic diversities are produced more rapidly by sequential infection than simultaneous infection via cell-to-cell transmission. To measure the relative contribution of both two infection modes on the growth of virions, Komarova et al. [21] fitted the existing model to experimental data and showed that the contributions of these two modes are comparable. In [22], Lai and Zou identified that the basic reproduction number of the proposed HIV-1 model are weighted by both virus-to-cell and cell-to-cell infection pathways. A general distributed delayed viral infection model involving these two transmission mechanisms were proposed to investigate the global stability dynamics and Hopf bifurcation [23].

In the majority prior mathematical models, the loss of virions when they access the healthy cells in the infection process was usually ignored. However, some existing works revealed that loss term of free viruses could have considerable biological interpretations [24–26]. The basic reproduction number, viral dynamics and the infected equilibrium change greatly between the omission and inclusion of the virus loss under certain conditions in [26]. HIV-induced immune activation may trigger the proliferation of immune cells and lead to the recruitment of $CD4^+$ T cells [27,28]. During the early stages of infection, HIV can trigger immune activation and inflammation, potentially leading to the production of cytokines such as Interleukin 2 (IL-2) and Interleukin 7 (IL-7). It has been suggested in [29,30] that treating with IL-2 and IL-7 can replenish the naïve $CD4^+$ T cell pool, thereby contributing to an increase in naïve $CD4^+$ T cell count. The T cells grow after encountering specific antigens [6,31], and once activated, they can stimulate other T cells regardless of their specificity to HIV [32]. A nonlinear term $rTV/(C+V)$ is commonly used to characterize the HIV-stimulated proliferation of $CD4^+$ T cells [28,32–34]. Motivated by the earlier works, a viral infection model incorporating two transmission modes, viral loss dynamics and the proliferation of healthy target cells stimulated by free viruses are constructed as follows:

$$\begin{aligned} T'(t) &= s - \mu_1 T(t) + \frac{rT(t)V(t)}{c+V(t)} - \beta_1 T(t)V(t) - \beta_2 T(t)I(t),\\ I'(t) &= \beta_1 T(t)V(t) + \beta_2 T(t)I(t) - \mu_2 I(t),\\ V'(t) &= kI(t) - \mu_3 V(t) - \alpha T(t)V(t). \end{aligned} \tag{1.1}$$

Here, $T(t)$, $I(t)$ and $V(t)$ are the concentrations of uninfected target cells, actively infected cells, and free viruses at time t, respectively. The healthy cells are produced from sources within the body, such as the thymus, at a constant rate s, die at a per capita rate μ_1, and are infected by free viruses and infected cells at a rate of $\beta_1 TV$ and $\beta_2 TI$, respectively. The parameter r denotes the maximal proliferation rate and c is the half saturation constant of the proliferation process. The viral particles are generated by infected cells at a rate kI. Parameters μ_2 and μ_3 are the per capita death rates of infected cells and free viruses, respectively. The bilinear term αTV describes the loss term of virions when they encounter uninfected target cells. All parameters of model (1.1) are assumed to be positive.

We arrange the rest of this paper as follows. In Section 2, we present preliminary results interpreting the nonnegativity and boundedness of the solutions of (1.1), as well as the existence conditions of equilibria. Local and global asymptotic stability analyses of equilibria are formulated in Section 3. In Section 4, we explore the effects of two key parameters on the stability dynamics and conduct Hopf bifurcation examination. Numerical simulations are carried out to show the applicability of our theoretical results and reveal rich bifurcation dynamics in Section 5. Finally, we briefly summarize the main results and discuss future work in Section 6.

2. Preliminaries and basic dynamics

In this section, we investigate the well-posedness of model (1.1). Let $\phi(t,t_0,\phi_0)$ be the solution of (1.1) with the initial condition $\phi_0 = (T_0, I_0, V_0) \in \mathbb{R}^3_+$ at $t = t_0$.

Theorem 2.1. *System (1.1) with nonnegative initial condition ϕ_0 at $t = t_0$ admits a unique global solution $\phi(t,t_0,\phi_0)$ that is nonnegative for $t \geq 0$. Furthermore, if $r < (\sqrt{\mu_1} + \sqrt{\beta_1 c})^2$, then solutions are ultimately uniformly bounded in $\mathbb{R}^3_+$.*

Proof. The local existence and uniqueness of the solution follow from the standard theory of ordinary differential equations. The nonnegativeness of the solution can be proved by a simple contradictory argument.

Now, we denote by $t_{max} > 0$ the largest time for the existence of solution; namely, the solution exists for all $t \in [0, t_{max})$, and either $t_{max} = \infty$ or the solution blows up as $t \to t^-_{max}$. We claim that the second case is impossible. Otherwise, assuming $t_{max} < \infty$, we obtain from the nonnegativeness of the solution and a linear combination of the three equations in (1.1) that

$$\begin{aligned} T'(t) + I'(t) + V'(t) &\leq s + rT(t) + kI(t)\\ &\leq s + (r+k)[T(t) + I(t) + V(t)], \end{aligned}$$

which implies $T(t) + I(t) + V(t)$ are uniformly bounded by a constant depending on the initial values and t_{max} for all $t \in [0, t_{max})$, a contradiction to the assumption that $T(t) + I(t) + V(t) \to \infty$ as $t \to t^-_{max}$. This proves the global existence of the solution.

Assume $r < \check{r} := (\sqrt{\mu_1} + \sqrt{\beta_1 c})^2$. Define $g_1(V) = rV/(c+V) - \beta_1 V$. Obviously,

$$\max_{V \geq 0} g_1(V) = \begin{cases} 0, & r \in (0, \beta_1 c],\\ (\sqrt{r} - \sqrt{\beta_1 c})^2, & r \in (\beta_1 c, \check{r}). \end{cases}$$

Denote $\hat{\mu}_1 = \mu_1 - \max_{V \geq 0} g_1(V)$, then

$$\hat{\mu}_1 = \begin{cases} \mu_1, & r \in (0, \beta_1 c],\\ \mu_1 - (\sqrt{r} - \sqrt{\beta_1 c})^2, & r \in (\beta_1 c, \check{r}). \end{cases}$$

Since $r < \check{r}$, we have $\hat{\mu}_1 > 0$. It then follows from the first equation of (1.1) that

$$T'(t) = s - \mu_1 T + g_1(V)T - \beta_2 TI \leq s - \hat{\mu}_1 T.$$

Thus, $\limsup_{t\to\infty} T(t) \leq \overline{T} := \frac{s}{\hat{\mu}_1}$. There exists $t_1 > 0$ such that $T(t) < \overline{T} + 1$ for all $t \geq t_1$. Adding the first two equations of (1.1) gives

$$\begin{aligned} (T(t) + I(t))' &= s - \mu_1 T(t) + \frac{rT(t)V(t)}{c+V(t)} - \mu_2 I(t)\\ &\leq s + r(\overline{T} + 1) - \min\{\mu_1, \mu_2\}(T(t) + I(t)), \end{aligned}$$

for all $t \geq t_1$. Then $\limsup_{t\to\infty}(T(t) + I(t)) \leq \overline{I} := \frac{s + r(\overline{T}+1)}{\min\{\mu_1, \mu_2\}}$. Hence, there exists $t_2 > t_1$ such that $T(t) + I(t) < \overline{I} + 1$ for all $t \geq t_2$. This, together with the third equation of (1.1), implies that $V'(t) \leq k(\overline{I} + 1) - \mu_3 V(t)$ for all $t \geq t_2$. Hence, $\limsup_{t\to\infty} V(t) \leq \overline{V} := \frac{k(\overline{I}+1)}{\mu_3}$. The proof is completed. □

System (1.1) admits a unique infection free equilibrium (IFE) $E_0 = (T_0, 0, 0)$, where $T_0 = s/\mu_1$. It may also have infection persistent equilibrium (IPE) $E^* = (T^*, I^*, V^*)$, where T^* is the unique positive zero of the quadratic polynomial

$$f(T) = \alpha\beta_2 T^2 + (k\beta_1 + \mu_3\beta_2 - \mu_2\alpha)T - \mu_2\mu_3, \tag{2.1}$$

given by

$$T^* = \frac{\mu_2\alpha - k\beta_1 - \mu_3\beta_2 + \sqrt{(k\beta_1 + \mu_3\beta_2 - \mu_2\alpha)^2 + 4\alpha\beta_2\mu_2\mu_3}}{2\alpha\beta_2},$$

and V^* is the positive zero of another quadratic polynomial

$$g(V) = V^2 + (p_1 - p_2 + c)V + p_1 c, \tag{2.2}$$

where

$$p_1 = \frac{k\mu_1(T^* - T_0)}{\mu_2(\mu_3 + \alpha T^*)},\quad p_2 = \frac{krT^*}{\mu_2(\mu_3 + \alpha T^*)}.$$

It follows from the third equation of (1.1) that

$$I^* = \frac{(\mu_3 + \alpha T^*)V^*}{k}. \tag{2.3}$$

Denote

$$R(T) = \frac{k\beta_1 T}{\mu_2(\mu_3 + \alpha T)} + \frac{\beta_2 T}{\mu_2},$$

then we can conclude from the expression of T^* that $R(T^*) = 1$. Using the next generation matrix method, the basic reproduction number of (1.1) can be directly calculated as follows:

$$R_0 = R(T_0) = \frac{k\beta_1 s}{\mu_2(\mu_1\mu_3 + \alpha s)} + \frac{\beta_2 s}{\mu_1\mu_2}. \tag{2.4}$$

Note that $f(T_0) = \mu_2(\mu_3 + \alpha T_0)(R_0 - 1)$ and $f(T^*) = 0$. Integrating these equations with p_1 leads to

$$\text{Sign}\{p_1\} = \text{Sign}\{T^* - T_0\} = \text{Sign}\{1 - R_0\}. \tag{2.5}$$

Next, we study the existence of the IPE. If $R_0 > 1$, that is $p_1 < 0$, $g(V)$ possesses a unique positive zero, then model (1.1) admits a unique IPE E^*. If $R_0 = 1$, then there exists a unique E^* if and only if $r > \bar{r}$, where

$$\bar{r} = \frac{c\mu_2(\mu_3 + \alpha T^*)}{kT^*} > \beta_1 c. \tag{2.6}$$

If $R_0 < 1$, then model (1.1) have two IPE following $E_1^* = (T^*, I_1^*, V_1^*)$ and $E_2^* = (T^*, I_2^*, V_2^*)$, provided that $p_1 - p_2 + c < 0$ and $\bar{p} = (p_1 - p_2 + c)^2 - 4p_1 c > 0$, where

$$V_1^* = \frac{p_2 - p_1 - c + \sqrt{\bar{p}}}{2},\ V_2^* = \frac{p_2 - p_1 - c - \sqrt{\bar{p}}}{2}. \tag{2.7}$$

Additionally, a convergence of these two IPE occurs when $\bar{p} = 0$, which is equivalent to $R_0 = 1 - \xi$, where

$$\xi = \frac{\mu_2\mu_3 + \alpha\beta_2 T_0 T^*}{\mu_1\mu_2(\mu_3 + \alpha T_0)}\left(\sqrt{r} - \sqrt{\bar{r}}\right)^2. \tag{2.8}$$

For convenience, we also denote

$$\hat{r} := \left(\sqrt{\bar{r}} + \sqrt{\frac{\mu_1\mu_2(\mu_3 + \alpha T_0)}{\mu_2\mu_3 + \alpha\beta_2 T_0 T^*}}\right)^2 > \bar{r}. \tag{2.9}$$

It then follows that $\xi \geq 1$ when $r \geq \hat{r}$ and $\xi \in (0, 1)$ when $r \in (\bar{r}, \hat{r})$.

The existence of equilibria of model (1.1) can be categorized as follows.

Lemma 2.1. *Let R_0, $\bar{r}$, ξ, and $\hat{r}$ be defined in (2.4), (2.6), (2.8), and (2.9), respectively. Considering system (1.1), the IFE E_0 always exists.*

(i) *Assume $r \leq \bar{r}$. If $R_0 \leq 1$, then the IFE E_0 is the unique equilibrium. If $R_0 > 1$, then besides E_0, system (1.1) admits a unique IPE E^*.*

(ii) *Assume $r \in (\bar{r}, \hat{r})$. If $R_0 < 1 - \xi$, then the IFE E_0 is the unique equilibrium. If $R_0 \in (1 - \xi, 1)$, then besides E_0, system (1.1) admits two IPE $E_1^* = (T^*, I_1^*, V_1^*)$ and $E_2^* = (T^*, I_2^*, V_2^*)$ with $V_1^* > V_2^*$. If either $R_0 = 1 - \xi$ or $R_0 \geq 1$, then besides E_0, system (1.1) admits a unique IPE.*

(iii) *Assume $r \geq \hat{r}$. If $R_0 < 1$, then besides E_0, system (1.1) admits two IPE $E_1^* = (T^*, I_1^*, V_1^*)$ and $E_2^* = (T^*, I_2^*, V_2^*)$ with $V_1^* > V_2^*$. If $R_0 \geq 1$, then besides E_0, system (1.1) admits a unique IPE.*

3. Stability analysis

3.1. Stability analysis of the IFE

We now explore the stability of the IFE E_0. By analyzing the root distribution in the characteristic equation and employing the center manifold theory, we establish the local asymptotic stability of E_0.

Theorem 3.1. *Consider system (1.1).*

(i) *If $R_0 < 1$, then the IFE E_0 is locally asymptotically stable.*

(ii) *If $R_0 > 1$, then the IFE E_0 is unstable.*

(iii) *If $R_0 = 1$, then the IFE E_0 is locally asymptotically stable when $r \leq \bar{r}$, but E_0 is unstable when $r > \bar{r}$.*

Proof. Linearizing system (1.1) at $E_0 = (T_0, 0, 0)$ gives the characteristic equation $(\lambda + \mu_1)F_0(\lambda) = 0$ with

$$F_0(\lambda) = \lambda^2 + \left(\frac{k\beta_1 T_0}{\mu_3 + \alpha T_0} + \mu_3 + \alpha T_0 - \mu_2(R_0 - 1)\right)\lambda - \mu_2(\mu_3 + \alpha T_0)(R_0 - 1).$$

If $R_0 > 1$, then there exists a positive eigenvalue, indicating that E_0 is unstable. If $R_0 < 1$, then all eigenvalues have negative real parts, thus E_0 is locally asymptotically stable. If $R_0 = 1$, then there are two negative eigenvalues and a simple eigenvalue of 0. We can then analyze the local stability of E_0 using the center manifold theory and normal form. Let

$$\omega(t) = (\omega_1(t), \omega_2(t), \omega_3(t))^T = (T(t) - T_0, I(t), V(t))^T,$$

then model (1.1) can be rewritten as

$$\dot{\omega} = A\omega + F(\omega), \tag{3.1}$$

where

$$A = \begin{pmatrix} -\mu_1 & -\beta_2 T_0 & rT_0/c - \beta_1 T_0 \\ 0 & -\mu_2 + \beta_2 T_0 & \beta_1 T_0 \\ 0 & k & -\mu_3 - \alpha T_0 \end{pmatrix},$$

and

$$F(\omega) = \begin{pmatrix} -\beta_1\omega_1\omega_3 - \beta_2\omega_1\omega_2 + \dfrac{r\omega_3(c\omega_1 - T_0\omega_3)}{c(c + \omega_3)} \\ \beta_1\omega_1\omega_3 + \beta_2\omega_1\omega_2 \\ -\alpha\omega_1\omega_3 \end{pmatrix}.$$

The right and left eigenvectors of the linear matrix A with respect to $\lambda = 0$ are $q = (q_1, q_2, 1)^T$ and $q^* = Q(0, 1, q_3^*)$, respectively, and

$$\begin{aligned} q_1 &= \frac{krT_0 - c\mu_2(\mu_3 + \alpha T_0)}{ck\mu_1},\ q_2 = \frac{\mu_3 + \alpha T_0}{k}, \\ Q &= \frac{k}{\mu_2 - \beta_2 T_0 + \mu_3 + \alpha T_0},\ q_3^* = \frac{\mu_2 - \beta_2 T_0}{k}, \end{aligned} \tag{3.2}$$

where the constant Q is chosen such that the inner product $\langle q^*, q\rangle = 1$. Since $R_0 = 1$, we obtain from (2.4) that

$$\mu_2 - \beta_2 T_0 = \frac{k\beta_1 T_0}{\mu_3 + \alpha T_0} > 0,$$

and consequently, $Q > 0$ and $q_3^* > 0$. Following [35, Section 5.4.1], we let $\omega = xq + y$ such that $\langle q^*, y\rangle = 0$, where $x = \langle q^*, \omega\rangle$ is small, and $y = ax^2 + O(x^3)$ with $a = (a_1, a_2, a_3)^T$; see [36, Theorem 2.12.1]. Since $\omega_3 > 0$ for all $t > 0$, we have $x > 0$ for all $t > 0$. By taking derivatives with respect to t, we obtain from (3.1), $Aq = 0$ and $q^*A = 0$ that $\dot{x} = \langle q^*, \dot{\omega}\rangle = \langle q^*, F(xq + y)\rangle$. A simple calculation gives the normal form

$$\dot{x} = \frac{k\beta_1\mu_3 + \beta_2(\mu_3 + \alpha T_0)^2}{k\beta_1 T_0 + (\mu_3 + \alpha T_0)^2} q_1 x^2 + Q\varphi x + O(x^4)$$

with $\varphi = (\beta_1 - q_3^*\alpha)(q_1 y_3 + y_1) + \beta_2(q_1 y_2 + q_2 y_1) = O(x^2)$. If $q_1 < 0$, then the IFE E_0 is locally asymptotically stable. If $q_1 > 0$, then E_0 is unstable.

Now, we consider the critical case $q_1 = 0$. Since $y_1 = a_1 x^2 + O(x^3)$, we have

$$\dot{x} = \frac{k\beta_1\mu_3 + \beta_2(\mu_3 + \alpha T_0)^2}{k(\mu_3 + \alpha T_0)} Q a_1 x^3 + O(x^4). \tag{3.3}$$

The stability of x is determined by the sign of a_1. To compute a_1, we first note from $y = ax^2 + O(x^3)$ and $\dot{x} = O(x^3)$ that $\dot{y} = O(x^4)$. Then, we obtain from $y = w - xq = w - \langle q^*, \omega\rangle q$ and (3.1) that

$$\dot{y} = \dot{\omega} - \langle q^*, \dot{\omega}\rangle q = Ay + F(xq + y) - \langle q^*, F(xq + y)\rangle q.$$

Since $q_1 = 0$, we further calculate $\dot{y} = (Aa + \rho)x^2 + O(x^3)$ with $\rho = (-rT_0/c^2, 0, 0)^T$. Coupling this with $\dot{y} = O(x^4)$ yields $Aa + \rho = 0$. Recall

that A is not invertible and $Aq = 0$, where $q = (q_1, q_2, 1)^T$ with $q_1 = 0$. A particular solution to the equation $Au + \rho = 0$ is $u = (u_1, 0, 0)^T$ with $u_1 = -rT_0/(c^2\mu_1) < 0$. The general solution to the equation $Aa + \rho = 0$ is given by $a = u + c_0 q$ with c_0 being an arbitrary constant. Since $q_1 = 0$, we have $a_1 = u_1 + c_0 q_1 = -rT_0/(c^2\mu_1) < 0$. Substituting this term into (3.3) yields

$$\dot{x} = -\frac{QrT_0\left[k\beta_1\mu_3 + \beta_2(\mu_3 + \alpha T_0)^2\right]}{kc^2\mu_1(\mu_3 + \alpha T_0)}x^3 + O(x^4),$$

which implies that E_0 is locally asymptotically stable.

Finally, we come back to the case $q_1 \neq 0$. Note from (2.5), (2.6) and (3.2) that $T^* = T_0$ and $\mathrm{Sign}\{q_1\} = \mathrm{Sign}\{r - \bar{r}\}$. Therefore, E_0 is locally asymptotically stable if $r \leq \bar{r}$ and unstable if $r > \bar{r}$. The proof is completed. □

By employing the LaSalle invariance principle, we proceed to analyze the global asymptotic stability of the IFE E_0.

Theorem 3.2. *Assume that $r \leq \beta_1 c$ and $R_0 \leq 1$, then the IFE E_0 is globally asymptotically stable in $\mathbb{R}^3_+$.*

Proof. Since $r \leq \beta_1 c$, we obtain from the nonnegativeness of the solution and the first equation in (1.1) that $T'(t) \leq s - \mu_1 T(t)$. It follows from the comparison principle that

$$\limsup_{t\to\infty} T(t) \leq \frac{s}{\mu_1} = T_0.$$

Now, we restrict (1.1) on the invariant set $D := [0, T_0] \times [0, \infty) \times [0, \infty)$ and construct the Lyapunov function

$$L(u_1, u_2, u_3) = u_1 - T_0 \ln u_1 + (1 + \frac{\alpha T_0}{\mu_3})u_2 + \frac{\beta_1 T_0}{\mu_3}u_3$$

for $u = (u_1, u_2, u_3) \in D$. Let $\{T(t), I(t), V(t)\}$ be any solution of (1.1) in D. A simple calculation yields

$$\begin{aligned}\dot{L}(T, I, V) = {} & \mu_1\left(1 - \frac{T_0}{T}\right)(T_0 - T) + \frac{rV}{c + V}(T - T_0) \\ & + \left(\frac{\alpha\beta_2 T_0 T}{\mu_3} + \beta_2 T_0 + \frac{k\beta_1 T_0}{\mu_3} - \mu_2 - \frac{\alpha\mu_2 T_0}{\mu_3}\right) I.\end{aligned}$$

We obtain from $T \leq T_0$ and $(1 - T_0/T)(T_0 - T) \leq 0$ that

$$\dot{L}(T, I, V) \leq \left(\frac{\beta_2 T_0(\mu_3 + \alpha T_0) + k\beta_1 T_0}{\mu_3} - \mu_2 - \frac{\alpha\mu_2 T_0}{\mu_3}\right) I.$$

Since

$$R_0 = \frac{k\beta_1 T_0}{\mu_2(\mu_3 + \alpha T_0)} + \frac{\beta_2 T_0}{\mu_2} \leq 1,$$

we have

$$\frac{\beta_2 T_0(\mu_3 + \alpha T_0) + k\beta_1 T_0}{\mu_3} \leq \frac{\mu_2(\mu_3 + \alpha T_0)}{\mu_3} = \mu_2 + \frac{\alpha\mu_2 T_0}{\mu_3},$$

and hence $\dot{L}(T, I, V) \leq 0$. It then follows from LaSalle invariance principle that $E_0 = (T_0, 0, 0)$ is globally attractive in D. Given any nonnegative initial value, by [37, Lemma 1.2.1], the corresponding omega limit set is internally chain transitive. Since D absorbs this initial value and contains its omega limit set, we obtain from [37, Theorem 1.2.1] that E_0 attracts all solutions initiating from nonnegative initial values. This together with the local asymptotic stability of E_0 implies that E_0 is globally asymptotically stable. □

3.2. Stability analysis of the IPE

We next investigate the stability of the IPE. The Jacobian matrix of (1.1) at $E^* = (T^*, I^*, V^*)$ is

$$J^* = \begin{pmatrix} \zeta & -\beta_2 T^* & \frac{rcT^*}{(c + V^*)^2} - \beta_1 T^* \\ \beta_1 V^* + \beta_2 I^* & -\mu_2 + \beta_2 T^* & \beta_1 T^* \\ -\alpha V^* & k & -\mu_3 - \alpha T^* \end{pmatrix}$$

with $\zeta = -\mu_1 + rV^*/(c + V^*) - \beta_1 V^* - \beta_2 I^*$. Then the characteristic equation of the linearized system of (1.1) at E^* is

$$\Delta(\lambda) = \lambda^3 + b_2\lambda^2 + b_1\lambda + b_0, \tag{3.4}$$

where

$$\begin{aligned} b_2 &= \frac{s}{T^*} + \frac{k\beta_1 T^*}{\mu_3 + \alpha T^*} + \mu_3 + \alpha T^* > 0, \\ b_1 &= \frac{s}{T^*}\left(\frac{k\beta_1 T^*}{\mu_3 + \alpha T^*} + \mu_3\right) + \alpha T^*\left(\mu_1 - \frac{rV^{*2}}{(c + V^*)^2}\right) \\ &\quad + \beta_2 I^*(\mu_2 + \alpha T^*), \\ b_0 &= (\mu_2\mu_3 + \alpha\beta_2 T^{*2})\left(\frac{\mu_1}{T^*}(T_0 - T^*) + \frac{rV^{*2}}{(c + V^*)^2}\right). \end{aligned}$$

Then a tedious calculation yields

$$\begin{aligned} b_1 b_2 - b_0 = {} & \frac{s}{T^*}\left[k_0^2 + (\mu_3 + k_0)\left(\mu_3 + \alpha T^* + \frac{s}{T^*}\right)\right. \\ & \left. + \beta_2 I^*(\mu_2 + \alpha T^*)\right] + \beta_1\beta_2 T^* V^*(\mu_2 + \alpha T^*) \\ & + \beta_2 T^*(\mu_3 + \alpha T^*)\left(\alpha I^* + \frac{rcV^*}{(c + V^*)^2}\right) \\ & + k_1\left(\mu_1 - \frac{rV^{*2}}{(c + V^*)^2}\right), \end{aligned}$$

where $k_0 = k\beta_1 T^*/(\mu_3 + \alpha T^*)$ and $k_1 = \alpha^2 T^{*2} + (\mu_3\alpha + k\beta_1)T^* + \alpha s$. To ensure the stability of E^*, we temporarily assume that $r \leq \mu_1$. Then the local asymptotic stability results of the IPE can be described as follows.

Theorem 3.3. *Consider system (1.1) with $r \leq \mu_1$. Let $V_1^* > V_2^*$ be defined in (2.7).*

(i) *Assume $r \leq \bar{r}$ and $R_0 > 1$, then the unique IPE E^* is locally asymptotically stable.*

(ii) *Assume $r \in (\bar{r}, \hat{r})$.*

(ii.1) *If $R_0 \geq 1$, then the unique IPE is locally asymptotically stable.*

(ii.2) *If $R_0 \in (1 - \xi, 1)$, then $E_1^* = (T^*, I_1^*, V_1^*)$ is locally asymptotically stable and $E_2^* = (T^*, I_2^*, V_2^*)$ is unstable.*

(ii.3) *If $R_0 = 1 - \xi$, then the unique IPE is a saddle–node. A saddle–node bifurcation occurs at $R_0 = 1 - \xi$.*

(iii) *Assume $r \geq \hat{r}$.*

(iii.1) *If $R_0 \geq 1$, then the unique IPE is locally asymptotically stable.*

(iii.2) *If $R_0 < 1$, then $E_1^* = (T^*, I_1^*, V_1^*)$ is locally asymptotically stable and $E_2^* = (T^*, I_2^*, V_2^*)$ is unstable.*

Proof. Since $r \leq \mu_1$, we have $b_1 > 0$ and $b_1 b_2 - b_0 > 0$. If $R_0 \geq 1$, it then follows from (2.5) that $T_0 \geq T^*$, which indicates $b_0 > 0$. By Routh–Hurwitz criterion, all eigenvalues of (3.4) have negative real parts. Therefore, the unique IPE E^* is locally asymptotically stable when either $R_0 = 1, r > \bar{r}$ or $R_0 > 1$. This proves (i), (ii.1), and (iii.1).

Next, we investigate the stability of two IPE $E_1^* = (T^*, I_1^*, V_1^*)$ and $E_2^* = (T^*, I_2^*, V_2^*)$. If $r \in (\bar{r}, \hat{r})$ and $R_0 \in (1 - \xi, 1)$, then we obtain from Lemma 2.1 that $\bar{p} > 0$; namely,

$$\sqrt{p_1} < \sqrt{p_2} - \sqrt{c}. \tag{3.5}$$

We regard $b_0 = b_0(V^*)$ as an increasing function of V^*. It is easily seen that $b_0(V_b) = 0$, where

$$V_b = \frac{c}{p_2 - p_1}\left(p_1 + \sqrt{p_1 p_2}\right) > 0. \tag{3.6}$$

By (2.2) and (3.5), we have

$$\begin{aligned} g(V_b) &= \frac{c\sqrt{p_1 p_2}}{(p_2 - p_1)^2}\left(c(\sqrt{p_1} + \sqrt{p_2})^2 - (p_2 - p_1)^2\right) \\ &< \frac{c\sqrt{p_1 p_2}}{(p_2 - p_1)^2}\left(c(2\sqrt{p_2} - \sqrt{c})^2 - c(2\sqrt{p_2} - \sqrt{c})^2\right) \\ &= 0. \end{aligned}$$

This together with $g(V_1^*) = g(V_2^*) = 0$ implies that $V_2^* < V_b < V_1^*$. In view of the monotonicity of b_0 with respect to V^*, we then obtain $b_0(V_2^*) < 0 < b_0(V_1^*)$. By Routh–Hurwitz criterion, E_1^* is locally asymptotically stable, and E_2^* is unstable. This proves (ii.2). Similarly, we can also prove (iii.2) by verifying (3.5) and $b_0(V_2^*) < 0 < b_0(V_1^*)$.

Finally, we consider the critical case when $R_0 = 1 - \xi$. Now, we have $g(V_b) = 0$, $V^* = V_b = \sqrt{p_1 c}$, and hence, $b_0 = 0$. This together with $R(T^*) = 1$ implies $rcT^*/(c+V^*)^2 = \mu_2(\mu_3+\alpha T^*)/k$. Recall that $b_1 > 0$ and $b_2 > 0$. Therefore, 0 is a simple zero of the cubic polynomial in (3.4), while the other two zeros have negative real parts. We now employ Sotomayor's theorem [36, Theorem 4.2.1] to show that a saddle–node bifurcation appears at the IPE E^* when R_0 passes through the critical value $1 - \xi$. Without loss of generality, we choose k as the bifurcation parameter and denote by k_c the critical value of k when $R_0 = 1-\xi$. We calculate the right and left eigenvectors of the Jacobian matrix J^* with respect to the eigenvalue $\lambda = 0$ as $w = (0, 1, w_3)^T$ and $w^* = (w_1^*, 1, w_3^*)$, respectively, where

$$w_3 = \frac{k}{\mu_3 + \alpha T^*},\ w_1^* = \frac{kT^*\left(\beta_2\alpha T^* I^* + \mu_3(\beta_1 V^* + \beta_2 I^*)\right)}{(\mu_3 + \alpha T^*)(ks + \beta_2\alpha T^{*^2} V^*)},$$

$$w_3^* = \frac{\beta_2 T^{*^2}(\beta_1 V^* + \beta_2 I^*)(\mu_3 + \alpha T^*) + ks\beta_1 T^*}{(\mu_3 + \alpha T^*)(ks + \beta_2\alpha T^{*^2} V^*)}.$$

Denote the right-hand side equation of (1.1) by $F(T, I, V)$. One can show that $F_k(E^*, k_c) = (0, 0, I^*)^T$ and

$$D^2F(E^*, k_c)(w, w) = \left(-\frac{2rcT^* w_3^2}{(c+V^*)^3}, 0, 0\right)^T.$$

Thus, we have $w^* F_k(E^*, k_c) = w_3^* I^* \neq 0$ and

$$w^*[D^2F(E^*, k_c)(w, w)] = -\frac{2rcT^* w_3^2 w_1^*}{(c+V^*)^3} \neq 0.$$

By Sotomayor's theorem [36, Theorem 4.2.1], system (1.1) undergoes a saddle–node bifurcation at E^* when k crosses the critical value k_c. By using a similar calculation as in the proof of Theorem 3.1, we find the normal form of (1.1) at E^* as

$$\dot{x} = -\frac{rcT^* w_3^2 w_1^*}{(c+V^*)^3}x^2 + O(x^3).$$

By [36, Theorem 2.11.1], the unique IPE is a saddle–node. This proves (ii.3). □

Remark 3.1. If $r > \mu_1$, one can still proceed similarly as in the proof of Theorem 3.3 and show that $b_0(V_2^*) < 0$. This implies that the IPE E_2^* is always unstable whenever it exists. Specifically, E_2^* is a saddle with two-dimensional stable manifold and one-dimensional unstable manifold.

We then establish the global asymptotic stability of the infection persistent equilibrium by employing the geometric approach introduced by Li and Muldowney [38,39]. Consider the autonomous system of an ordinary differential equation

$$x'(t) = f(x), \quad x \in G,\ f \in C^1(G), \tag{3.7}$$

where $f : G \to \mathbb{R}^n$, G is an open set and simply connected in $\mathbb{R}^n$. Let x^* be an equilibrium of (3.7) and $x(t, x_0)$ be the solution of (3.7) such that $x(0, x_0) = x_0$. Assume that the following assumptions are satisfied.

($\mathbf{H_1}$) There exists a compact absorbing set $K \in G$.

($\mathbf{H_2}$) System (3.7) admits a unique equilibrium x^* in G.

If ($\mathbf{H_1}$) and ($\mathbf{H_2}$) hold, it then follows from [39, Theorem 3.5] that x^* is globally stable in G provided that system (3.7) satisfies the Bendixson criterion, which precludes the existence of nonconstant periodic solutions. Let $Q(x) \in C^1(G)$ be a $\binom{n}{2} \times \binom{n}{2}$ matrix-valued function and define

$$M = Q_f Q^{-1} + QJ^{[2]}Q^{-1},$$

where Q_f is obtained by replacing each entry q_{ij} of Q by its derivative in the direction of f. The matrix $J^{[2]}$ is the second additive compound matrix of the Jacobian matrix $J = Df(x)$ [40]. For $n = 3$, we have

$$J^{[2]} = \begin{pmatrix} J_{11}+J_{22} & J_{23} & -J_{13} \\ J_{32} & J_{11}+J_{33} & J_{12} \\ -J_{31} & J_{21} & J_{22}+J_{33} \end{pmatrix}. \tag{3.8}$$

Let $|\cdot|$ be a vector norm in $\mathbb{R}^n$ and the induced matrix norm in $\mathbb{R}^{n\times n}$. For a matrix $A \in \mathbb{R}^{n\times n}$, the Lozinskiĭ measure [41] with respect to $|\cdot|$ is

$$\xi(A) = \lim_{h\to 0^+} \frac{|I + hA| - 1}{h}.$$

Define

$$\bar{q}_2 = \limsup_{t\to\infty} \sup_{x_0\in K} \frac{1}{t}\int_0^t \xi(M(x(s, x_0)))ds. \tag{3.9}$$

By [39, Theorem 3.1], system (3.7) has no invariant simple closed rectifiable curve in G if $\bar{q}_2 < 0$.

Similarly to the manner of [34, Lemma 4.3], we can derive the uniform persistence result of (1.1) as follows.

Lemma 3.1. *If $R_0 > 1$, then there exists an $\epsilon > 0$ such that $\liminf_{t\to\infty} T(t) \geq \epsilon$, $\liminf_{t\to\infty} I(t) \geq \epsilon$, and $\liminf_{t\to\infty} V(t) \geq \epsilon$ for any solution of system (1.1) with initial condition in $\mathbb{R}^3_+$.*

Similarly to the proof of Theorem 2.1. Denote $\hat{I} = s(\mu_1 + r)/(\mu_1 \min\{\mu_1, \mu_2\})$, we can establish that if $r < \min\{\mu_1, \beta_1 c\}$, the region

$$\Gamma = \{(T, I, V) \in \mathbb{R}^3_+ : T \leq \frac{s}{\mu_1}, I \leq \hat{I}, V \leq \frac{k\hat{I}}{\mu_3}\} \tag{3.10}$$

is both positively invariant and absorbing in $\mathbb{R}^3_+$ with respect to system (1.1).

Theorem 3.4. *Let $\hat{I}$ be defined in (3.10) and $\eta = \min\{\mu_1 - r, \mu_2\}$. Assume $R_0 > 1$ and $r < \min\{\mu_1, \beta_1 c\}$, then the unique IPE E^* is globally asymptotically stable in $\mathbb{R}^3_+$ provided that $\hat{I} < \eta/\alpha$.*

Proof. $\mathring{\Gamma}$ is a simply connected region in $\mathbb{R}^3$. Then, it follows from Lemma 2.1 that system (1.1) has a unique IPE in $\mathring{\Gamma}$ if $R_0 > 1$, which implies ($\mathbf{H_2}$) holds. The uniform persistence of system (1.1), along with the boundedness of solutions given in Theorem 2.1, implies the existence of a compact absorbing set $K \in \mathring{\Gamma}$, that is, the assumption ($\mathbf{H_1}$) holds. Therefore, by Theorem 3.1 in [39], we only need to show that there exist a matrix-valued function $Q(x)$ and a Lozinskiĭ measure ξ such that $\bar{q}_2 < 0$. The Jacobian matrix of (1.1) is

$$J = \begin{pmatrix} \rho & -\beta_2 T & \frac{rcT}{(c+V)^2} - \beta_1 T \\ \beta_1 V + \beta_2 I & -\mu_2 + \beta_2 T & \beta_1 T \\ -\alpha V & k & -\mu_3 - \alpha T \end{pmatrix},$$

where $\rho = -\mu_1 + rV/(c+V) - \beta_1 V - \beta_2 I$. It then follows from (3.8) that the second additive compound matrix $J^{[2]}$ is

$$J^{[2]} = \begin{pmatrix} \rho - \mu_2 + \beta_2 T & \beta_1 T & -\frac{rcT}{(c+V)^2} + \beta_1 T \\ k & \rho - \mu_3 - \alpha T & -\beta_2 T \\ \alpha V & \beta_1 V + \beta_2 I & -\mu_2 + \beta_2 T - \mu_3 - \alpha T \end{pmatrix}.$$

Let $Q = Q(T(t), I(t), V(t)) = \mathrm{diag}\{1, I/V, I/V\}$, we obtain

$$Q_f Q^{-1} = \mathrm{diag}\left\{0, \frac{I'}{I} - \frac{V'}{V}, \frac{I'}{I} - \frac{V'}{V}\right\}.$$

Then

$$M = Q_f Q^{-1} + QJ^{[2]}Q^{-1} = \begin{pmatrix} M_{11} & M_{12} \\ M_{21} & M_{22} \end{pmatrix},$$

where

$$M_{11} = \rho - \mu_2 + \beta_2 T,\ M_{21} = \left(\frac{kI}{V}, \alpha I\right)^T,$$
$$M_{12} = \left(\frac{\beta_1 TV}{I}, \left(-\frac{rcT}{(c+V)^2} + \beta_1 T\right)\frac{V}{I}\right),$$

and

$$M_{22} = \begin{pmatrix} \rho + \delta & -\beta_2 T \\ \beta_1 V + \beta_2 I & -\mu_2 + \beta_2 T + \delta \end{pmatrix}$$

with $\delta = \frac{I'}{I} - \frac{V'}{V} - \mu_3 - \alpha T$. Let $(u, v, w) \in \mathbb{R}^3$ and take a norm $|(u, v, w)| = \max\{|u|, |v|+|w|\}$ in $\mathbb{R}^3$. Let ξ be the corresponding Lozinskiĭ measure. It then follows from [42] that

$$\xi(M) \le \max\{g_1, g_2\},$$

with $g_1 = \xi_1(M_{11})+|M_{12}|$, $g_2 = \xi_1(M_{22})+|M_{21}|$, $|M_{12}|$ and $|M_{21}|$ are the matrix norms with respect to the l_1 vector norm and ξ_1 is the Lozinskiĭ measure with respect to l_1 norm. Directly calculations yield

$$\xi_1(M_{11}) = \rho - \mu_2 + \beta_2 T,$$
$$|M_{12}| = \max\left\{\frac{\beta_1 TV}{I}, \left|-\frac{rc}{(c+V)^2} + \beta_1\right|\frac{TV}{I}\right\},$$
$$|M_{21}| = \frac{kI}{V} + \alpha I,$$
$$\xi_1(M_{22}) = \delta + \max\left\{-\mu_1 + \frac{rV}{c+V}, -\mu_2\right\}.$$

If $r \le \beta_1 c$, then $|M_{12}| = \beta_1 TV/I$. By (1.1), we have

$$\frac{I'}{I} = \frac{\beta_1 TV}{I} + \beta_2 T - \mu_2,\ \frac{V'}{V} = \frac{kI}{V} - \mu_3 - \alpha T.$$

Hence,

$$g_1 = \frac{I'}{I} - \mu_1 + \frac{rV}{c+V} - \beta_1 V - \beta_2 I \le \frac{I'}{I} - (\mu_1 - r),$$
$$g_2 = \frac{I'}{I} + \alpha I + \max\left\{-\mu_1 + \frac{rV}{c+V}, -\mu_2\right\}$$
$$\le \frac{I'}{I} + \alpha I - \min\{\mu_1 - r, \mu_2\}.$$

Recall $\eta = \min\{\mu_1 - r, \mu_2\}$. Thus

$$\xi(M) \le \frac{I'}{I} + \alpha I - \eta \le \frac{I'}{I} + \alpha \hat{I} - \eta, \tag{3.11}$$

where $\hat{I}$ is the upper bound of I given in (3.10). Let $(T(t), I(t), V(t))$ be any solution of (1.1) initiating in the compact absorbing set K and $\bar{t}$ be sufficiently large such that $(T(t), I(t), V(t)) \in K$ for any $t \ge \bar{t}$. Along each solution $(T(t), I(t), V(t)) \in K$, integrating both sides of (3.11) for $t > \bar{t}$, we obtain

$$\frac{1}{t}\int_0^t \xi(M(x(s, x_0)))ds \le \frac{1}{t}\int_0^{\bar{t}} \xi(M(x(s, x_0)))ds + \frac{1}{t}\ln\frac{I(t)}{I(\bar{t})} + \frac{t-\bar{t}}{t}(\alpha\hat{I} - \eta).$$

If $\hat{I} < \eta/\alpha$, then

$$\lim_{t\to\infty}\frac{1}{t}\int_0^t \xi(M(x(s, x_0)))ds \le \alpha\hat{I} - \eta < 0.$$

This indicates $\bar{q}_2 < 0$ by (3.9). Hence, system (1.1) has no nonconstant periodic solution. By [39, Theorem 3.5], the unique IPE E^* is globally asymptotically stable. □

4. Hopf bifurcation analysis

Theorem 3.3 suggests that the IPE E^* (or E_1^*) is locally asymptotically stable provided that $r \le \mu_1$, and the IPE E_2^* is unstable when it exists. Moreover, the stability of E^* is determined by the sign of $b_1 b_2 - b_0$, which may be negative if $r > \mu_1$. This implies that E^* may lose its stability. In this section, we assume $r > \mu_1$ to investigate the stability switches of E^* and the existence of Hopf bifurcation.

4.1. Effects of r on viral dynamics

To explore the effects of the viral stimulation on the proliferation of healthy T cells, we employ r as the bifurcation parameter to implement theoretical analyses and numerical simulations. It follows from (2.1) and (2.4) that T^* and R_0 are independent of r. By (2.7), we have

$$\frac{dV_1^*}{dr} = \frac{kT^*V_1^*}{\sqrt{\bar{p}}\mu_2(\mu_3 + \alpha T^*)} > 0,$$

and

$$\frac{dV_2^*}{dr} = -\frac{kT^*V_2^*}{\sqrt{\bar{p}}\mu_2(\mu_3 + \alpha T^*)} < 0.$$

Along with (2.3), then V_1^* and I_1^* increase as r increases, while V_2^* and I_2^* decrease as r increases.

Proposition 4.1.

(i) *If system (1.1) admits a unique IPE $E^* = (T^*, I^*, V^*)$, then I^* and V^* increase as r increases.*
(ii) *If system (1.1) admits two IPE $E_1^* = (T^*, I_1^*, V_1^*)$ and $E_2^* = (T^*, I_2^*, V_2^*)$, then I_1^* and V_1^* increase as r increases, while I_2^* and V_2^* decrease as r increases.*

We now investigate the effects of r on the existence of the IPE. If $r \le \bar{r}$, then a unique E^* exists only if $R_0 > 1$. If $r > \bar{r}$, it follows from (2.8) that $1 - \xi$ decreases as r increases. By Lemma 2.1, the threshold for the existence of the IPE is $1 - \xi - R_0$, which admits a unique positive zero with respect to r following

$$r_s = \frac{\mu_2(\mu_3 + \alpha T^*)}{kT^*}(\sqrt{p_1} + \sqrt{c})^2 > \bar{r}. \tag{4.1}$$

If $R_0 < 1$, then system (1.1) has no IPE for $r < r_s$ and two IPE E_1^*, E_2^* for $r > r_s$, see Fig. 1(a) and (b). By applying a similar manner described in Theorem 3.3, we obtain that a saddle–node bifurcation occurs at E^* as r passes through the bifurcation value r_s. If $R_0 = 1$, then system (1.1) has a unique IPE for $r > \bar{r}$. If $R_0 > 1$, then system (1.1) still admits a unique IPE for any positive r, see Fig. 1(c) and (d). In conclusion, we obtain the following results.

Theorem 4.1. *Let $\bar{r}$ and r_s be defined in (2.6) and (4.1), respectively.*

(i) *If $R_0 < 1$, then system (1.1) admits two IPE E_1^* and E_2^* for $r > r_s$. They collide together and a saddle–node bifurcation appears at $r = r_s$.*
(ii) *If $R_0 = 1$, then system (1.1) admits a unique IPE E^* for $r > \bar{r}$.*
(iii) *If $R_0 > 1$, then system (1.1) admits a unique IPE E^* for $r > 0$.*

Next, we examine the stability switches of the IPE E^* (or E_1^*) as r bifurcates. Recall $b_0 > 0$ by Theorem 3.3, then the necessary and sufficient condition for the existence of Hopf bifurcation at the IPE is $b^* := b_1 b_2 - b_0 = 0$ [43, Theorem 2]. If $R_0 < 1$ and $r = r_s$, then two IPE E_1^* and E_2^* collide with each other and $b_0(V_1^*) = b_0(V_2^*) = 0$ is satisfied, which implies $\mu_1 - rV^{*2}/(c+V^*)^2 = \mu_1 T_0/T^* > 0$. Hence, $b_1 > 0$ and further $b^*(r_s) > 0$. If $R_0 > 1$, then it is clearly observed from the expression of b^* that $b^*(0) > 0$ holds. If $R_0 = 1$ and $r = \bar{r}$, then Lemma 2.1 indicates $V^* = 0$. Denote the minimum value of r by r_m such that E^* (or E_1^*) can exist, then we have $b^*(r_m + \epsilon) > 0$ with a small positive constant ϵ by the continuity of b^* with respect to r. Therefore, the IPE E^* (or E_1^*) if exists is stable at first with the bifurcation parameter r increasing.

Numerical results show that a unique positive zero of b^* with respect to r exists such that $b^*(r_h) = 0$ under the given parameters space presented in Fig. 1. It holds $b^* > 0$ for $r < r_h$ and $b^* < 0$ for $r > r_h$, which leads to the appearance of Hopf bifurcation for (1.1) when r exceeds the Hopf bifurcation value r_h, see Fig. 1(a) and (c). In addition, the IPE becomes unstable together with stable limit cycles for $r > r_h$. Proposition 4.1 and Fig. 1 indicate that an increase in the proliferation

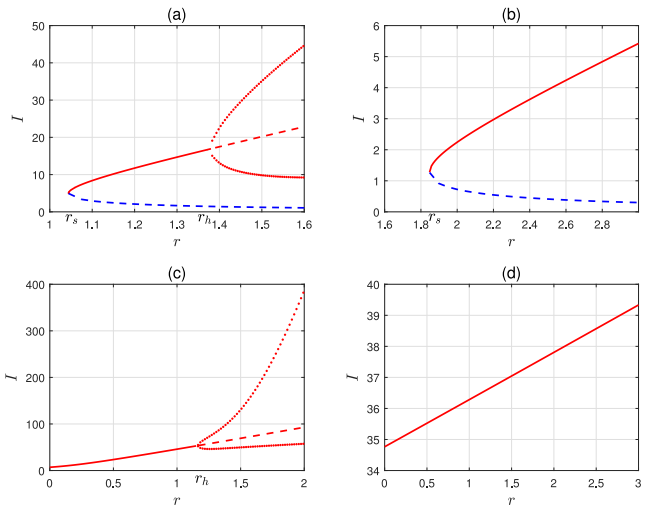


Fig. 1. Bifurcation diagram of infected cells with r as the bifurcation parameter. The parameters are: $c = 20$, $k = 40$, $\mu_1 = 0.6$, $\mu_2 = 0.28$, $\mu_3 = 2.4$ and (a) $s = 0.1$, $\beta_1 = 0.0008$, $\beta_2 = 0.03$, $\alpha = 0.13$; (b) $s = 0.1$, $\beta_1 = 0.0008$, $\beta_2 = 0.35$, $\alpha = 0.13$; (c) $s = 10$, $\beta_1 = 0.01$, $\beta_2 = 0.002$, $\alpha = 1.4$; (d) $s = 10$, $\beta_1 = 0.01$, $\beta_2 = 0.5$, $\alpha = 1.4$. The red solid (resp. dashed) line denotes the stable (resp. unstable) IPE E^* (or E_1^*), and the blue dashed line stands the unstable IPE E_2^*. The red points are the maximum and minimum values of the stable limit cycle. A saddle–node bifurcation occurs at $r = r_s$ and a Hopf bifurcation appears at $r = r_h$.

rate promotes the growth of infected cells and free viruses, potentially leading to sustained oscillatory dynamics when cell-to-cell infection intensity is low. Therefore, controlling the proliferation rate is crucial for effective viral prevention and control. If the contribution of cell-to-cell infection to the production of newly infected cells increases, then no Hopf bifurcation occurs, see Fig. 1(b) and (d). Moreover, numerical calculations directly obtain that $b^* > 0$ for any $r > r_s$ or $r > 0$. Our results suggest that cell-to-cell infection mechanism plays indeed a significant role in the process of HIV transmission. This implies that it is indispensable to weigh both two infection modes to acquire more accurate understandings of viral kinetics.

4.2. Effects of α on viral dynamics

In this subsection, we choose α as the bifurcation parameter to investigate the effects of loss term of virions on the dynamics of system (1.1). It is observed from (2.4) that R_0 is decreasing as α increases and $\lim_{\alpha\to\infty} R_0 = \beta_2 T_0/\mu_2$. If $\alpha = 0$, then

$$R_0 = \frac{T_0(k\beta_1 + \mu_3\beta_2)}{\mu_2\mu_3} := R_0^0. \tag{4.2}$$

If $R_0^0 \le 1$, then $R_0 < 1$ for any $\alpha > 0$. If $\beta_2 T_0/\mu_2 \le 1 < R_0^0$, then $R_0 > 1$ for $\alpha \in (0, \alpha_t)$ and $R_0 < 1$ for $\alpha > \alpha_t$ with

$$\alpha_t = \frac{\mu_2\mu_3(R_0^0 - 1)}{T_0(\mu_2 - \beta_2 T_0)}. \tag{4.3}$$

If $\beta_2 T_0 > \mu_2$, then $R_0 > 1$ for all $\alpha > 0$. Taking a derivative of T^* with respect to α we obtain

$$\frac{dT^*}{d\alpha} = \frac{T^{*2}(\mu_2 - \beta_2 T^*)}{\mu_2\mu_3 + \alpha\beta_2 T^{*2}}.$$

The second equation of (1.1) suggests $\mu_2 - \beta_2 T^* = \beta_1 T^* V^*/I^*$. Thus $dT^*/d\alpha > 0$, which implies that T^* increases as α increases. Moreover, we have $\lim_{\alpha\to\infty} T^* = \mu_2/\beta_2$ and further $\lim_{\alpha\to\infty} R_0 = T_0/T^*$. The following results show the variation of viral load with α increasing.

Theorem 4.2.

(i) *If system (1.1) admits a unique IPE $E^* = (T^*, I^*, V^*)$, then V^* decreases as α increases.*

(ii) *If system (1.1) admits two IPE $E_1^* = (T^*, I_1^*, V_1^*)$ and $E_2^* = (T^*, I_2^*, V_2^*)$, then V_1^* decreases and V_2^* increases as α increases, respectively.*

Proof. Taking derivatives of V_1^* and V_2^* with respect to α yields

$$\frac{dV_1^*}{d\alpha} = -\frac{V_1^*(p_1' - p_2') + p_1' c}{\sqrt{(p_1 - p_2 + c)^2 - 4p_1 c}}, \tag{4.4}$$

and

$$\frac{dV_2^*}{d\alpha} = \frac{V_2^*(p_1' - p_2') + p_1' c}{\sqrt{(p_1 - p_2 + c)^2 - 4p_1 c}}, \tag{4.5}$$

where p_1' and p_2' are the derivatives of p_1 and p_2 with respect to α, respectively. Given by

$$p_1' = \frac{k\mu_1 T^*\left[k\beta_1 T^{*2} + \mu_2(\mu_3 + \alpha T^*)(T_0 - T^*)\right]}{\mu_2(\mu_3 + \alpha T^*)^2(\mu_2\mu_3 + \alpha\beta_2 T^{*2})}, \tag{4.6}$$

and

$$p_2' = -\frac{kr\beta_2 T^{*3}}{\mu_2(\mu_3 + \alpha T^*)(\mu_2\mu_3 + \alpha\beta_2 T^{*2})} < 0. \tag{4.7}$$

If $p_1' \ge 0$, then by (4.4) and (4.7) we have $dV_1^*/d\alpha < 0$. Note that $p_1' > 0$ when $T_0 \ge T^*$, and p_1' may be negative if $T_0 < T^*$. It thus follows from (2.5) that $dV_1^*/d\alpha < 0$ holds when $R_0 \ge 1$. This proves (i).

Next, we show $V_1^*(p_1' - p_2') + p_1' c > 0$ if $p_1' < 0$, which implies that $R_0 < 1$ is satisfied. By Lemma 2.1, the coexistence of E_1^* and E_2^* leads to $p_1 - p_2 + c < 0$ and $\bar{p} > 0$. It follows from (2.1) that $k\beta_1 T^* = (\mu_2 - \beta_2 T^*)(\mu_3 + \alpha T^*)$. Substituting it into (4.6), we yield

$$p_1' - p_2' = \frac{kT^*\left[\mu_1\mu_2 T_0 + \beta_2 T^{*2}(r - \mu_1)\right]}{\mu_2(\mu_3 + \alpha T^*)(\mu_2\mu_3 + \alpha\beta_2 T^{*2})}. \tag{4.8}$$

If $r \ge \mu_1$, then $p_1' - p_2' > 0$. If $r < \mu_1$, it follows from $\beta_2 T^* \le \mu_2$ that

$$\mu_1\mu_2 T_0 + \beta_2 T^{*2}(r - \mu_1) \ge \mu_2\left(\mu_1(T_0 - T^*) + rT^*\right).$$

Note that $p_1 - p_2 + c < 0$ is equivalent to $\mu_1(T_0 - T^*) + rT^* > c\mu_2(\mu_3 + \alpha T^*)/k$, thus $p_1' - p_2' > 0$ still holds. By Theorem 3.3, we have $V_1^* > V_b$, which indicates $V_1^*(p_1' - p_2') + p_1' c > V_b(p_1' - p_2') + p_1' c := \widetilde{V}$. It then follows from (3.6) that $\widetilde{V}$ can be rearranged as

$$\widetilde{V} = \frac{c}{p_2 - p_1}\left[p_1' p_2 - p_1 p_2' + \sqrt{p_1 p_2}(p_1' - p_2')\right].$$

Clearly, $p_2 - p_1 > c$. By the expressions of p_i and p_i' $(i = 1, 2)$, we obtain

$$p_1' p_2 - p_1 p_2' = \frac{k^2\mu_1 r T_0 T^{*2}(\mu_2 - \beta_2 T^*)}{\mu_2^2(\mu_3 + \alpha T^*)^2(\mu_2\mu_3 + \alpha\beta_2 T^{*2})} > 0.$$

Thus $\widetilde{V} > 0$ and further $V_1^*(p_1' - p_2') + p_1' c > 0$. By (4.4), $dV_1^*/d\alpha < 0$ is satisfied.

We now verify that $dV_2^*/d\alpha > 0$ when $p_1' < 0$. Denote $\widehat{V} = -p_1' c/(p_1' - p_2') > 0$ and substitute $V = \widehat{V}$ into $g(V)$ yields

$$g(\widehat{V}) = \frac{c}{(p_1' - p_2')^2}\left[cp_1' p_2' + (p_1' - p_2')(p_1' p_2 - p_1 p_2')\right] > 0.$$

Note that $dV_1^*/d\alpha < 0$ implies $\widehat{V} < V_1^*$, together with $V_2^* < V_1^*$ and $g(\widehat{V}) > 0$ we directly obtain $\widehat{V} < V_2^*$. It thus follows from (4.5) that $dV_2^*/d\alpha > 0$. The proof is completed. □

Next, we explore how does α affect the existence of the infection persistent equilibrium. To this end, we consider three cases (i) $\mu_2 < \beta_2 T_0$; (ii) $\beta_2 T_0/\mu_2 \le 1 < R_0^0$; and (iii) $R_0^0 \le 1$. If $\mu_2 < \beta_2 T_0$, then $R_0 > 1$ for any $\alpha > 0$. By Lemma 2.1, a unique IPE always exists. If $\beta_2 T_0/\mu_2 \le 1 < R_0^0$, then $R_0 > 1$ for $\alpha \in (0, \alpha_t)$ and $R_0 \le 1$ for $\alpha \ge \alpha_t$ with α_t defined in (4.3). Consider $R_0 \le 1$, which implies $p_1 \ge 0$ by (2.5). If $R_0 = 1$, then a unique IPE exists provided that $p_2(\alpha_t) > c$. If $R_0 < 1$, then

two IPE exist if and only if $\hat{p}(\alpha) = p_1(\alpha) - p_2(\alpha) + c < 0$ and $\bar{p}(\alpha) > 0$ for $\alpha > \alpha_t$. Since $p_1(\alpha_t) = 0$, we obtain $\hat{p}(\alpha_t) < 0$ is equivalent to $p_2(\alpha_t) > c$, that is, $r > r_m$ with

$$r_m = \frac{c\mu_2(\mu_3 + \alpha_t T_t^*)}{kT_t^*}, \tag{4.9}$$

where

$$T_t^* = \frac{\mu_2\alpha_t - k\beta_1 - \mu_3\beta_2 + \sqrt{(k\beta_1 + \mu_3\beta_2 - \mu_2\alpha_t)^2 + 4\alpha_t\beta_2\mu_2\mu_3}}{2\alpha_t\beta_2}.$$

By (4.8), $\hat{p}(\alpha)$ increases as α increases when $\hat{p}(\alpha) < 0$. Then the continuity of $\hat{p}(\alpha)$ and $\lim_{\alpha\to\infty}\hat{p}(\alpha) = c$ suggest that a unique positive zero $\alpha = \alpha_p$ exists such that $\hat{p}(\alpha_p) = 0$.

Denote $\bar{p}'$ by the derivative of $\bar{p}(\alpha)$ with respect to α, then $\bar{p}' = 2\hat{p}(p_1' - p_2') - 4p_1'c$. We have shown in Theorem 4.2 that $\widehat{V} < V_2^*$ if E_2^* exists, which implies $\widehat{V} < -\hat{p}/2$, that is, $\hat{p}(p_1' - p_2') < 2p_1'c$. Hence, $\bar{p}' < 0$ holds. Note that $\bar{p}(\alpha_t) = (c - p_2(\alpha_t))^2 > 0$ and $\bar{p}(\alpha_p) = -4p_1(\alpha_p)c < 0$. Thus by the continuity and monotonicity of $\bar{p}(\alpha)$, there exists a unique positive zero $\alpha = \alpha_s$ such that

$$(p_1(\alpha_s) - p_2(\alpha_s) + c)^2 - 4p_1(\alpha_s)c = 0, \tag{4.10}$$

and $\alpha_t < \alpha_s < \alpha_p$ are satisfied. In addition, it holds $\bar{p} > 0$ for $\alpha \in (0, \alpha_s)$ and $\bar{p} < 0$ for $\alpha > \alpha_s$. Therefore, E_1^* and E_2^* coexist for $\alpha \in (\alpha_t, \alpha_s)$ and collide together at $\alpha = \alpha_s$ provided that $r > r_m$.

If $R_0^0 \le 1$, then $R_0 < 1$ for all $\alpha > 0$. Thus two IPE coexist for $\alpha \in (0, \alpha_s)$ if and only if $\hat{p}(0) < 0$ and $\bar{p}(0) > 0$, which can be rewritten as $p_2(0) > (\sqrt{p_1(0)} + \sqrt{c})^2$, that is, $r > r_n$ with

$$r_n = \frac{1}{kT_0^*}\left(\sqrt{k\mu_1(T_0^* - T_0)} + \sqrt{c\mu_2\mu_3}\right)^2 \tag{4.11}$$

and $T_0^* = \mu_2\mu_3/(k\beta_1 + \mu_3\beta_2)$. Hence, the existence of the infection persistent equilibrium with α as the bifurcation parameter can be described as follows.

Theorem 4.3. *Let R_0^0, α_t, α_s, $\bar{r}$, r_m, and r_n be defined in (4.2), (4.3), (4.10), (2.6), (4.9), and (4.11), respectively.*

(i) *If $\mu_2 < \beta_2 T_0$, then system (1.1) admits a unique IPE E^* for any $\alpha > 0$.*

(ii) *If $\beta_2 T_0/\mu_2 \le 1 < R_0^0$, we obtain the following results.*

(ii.1) *Assume $r \le r_m$, then system (1.1) admits a unique IPE E^* for $\alpha \in (0, \alpha_t)$.*

(ii.2) *Assume $r > r_m$, then system (1.1) admits E_1^* for $\alpha \in (0, \alpha_s)$ and E_2^* for $\alpha \in (\alpha_t, \alpha_s)$. Moreover, E_1^* and E_2^* collide together at $\alpha = \alpha_s$.*

(iii) *If $R_0^0 \le 1$ and $r > r_n$, then system (1.1) admits two IPE E_1^* and E_2^* for $\alpha \in (0, \alpha_s)$, and they collide together at $\alpha = \alpha_s$.*

Moreover, a transcritical bifurcation appears at $\alpha = \alpha_t$ provided that $r \ne \bar{r}$ and a saddle–node bifurcation occurs at $\alpha = \alpha_s$.

Proof. We have interpreted the existence of the infection persistent equilibrium with the bifurcation parameter α varying. Using a similar manner to Theorem 3.3, we can directly conclude that system (1.1) experiences a saddle–node bifurcation at the IPE when α passes through the bifurcation value α_s. It now suffices to demonstrate the appearance of transcritical bifurcation.

Note that $\alpha = \alpha_t$ indicates $R_0 = 1$, then $T_0 = T^*$ holds by (2.5). It thus follows from Theorem 3.1 that the characteristic equation of E_0 has two eigenvalues with negative real parts and a simple eigenvalue 0. We have shown in (3.2) that $q = (q_1, q_2, 1)^T$ and $q^* = Q(0, 1, q_3^*)$ are the right and left eigenvectors of the linear matrix A with respect to $\lambda = 0$, respectively. Directly calculation yields $F_\alpha(E_0, \alpha_t) = (0, 0, 0)^T$, $DF_\alpha(E_0, \alpha_t)q = (0, 0, -T_0)^T$ and

$$D^2F(E_0, \alpha_t)(q, q) = \begin{pmatrix} -\dfrac{2\hat{q}}{c^2} \\ 2q_1(\beta_1 + \beta_2 q_2) \\ -2\alpha_t q_1 \end{pmatrix}$$

with $\hat{q} = rT_0 + c^2\beta_2 q_1 q_2 + (c^2\beta_1 - cr)q_1$. Then we have

$$q^* F_\alpha(E_0, \alpha_t) = 0,\ q^*\left[DF_\alpha(E_0, \alpha_t)q\right] = -q_3^* Q T_0 \ne 0,$$

and

$$q^*\left[D^2F(E_0, \alpha_t)(q, q)\right] = \frac{2q_1 Q(\mu_2\mu_3 + \beta_2\alpha_t T_0^2)}{kT_0}.$$

Hence, by Sotomayor's theorem [36, Theorem 4.2.1], system (1.1) undergoes a transcritical bifurcation at the IFE E_0 as α passes through the bifurcation value α_t provided that $q_1 \ne 0$, that is, $r \ne \bar{r}$. □

We now investigate how does α affect the stability of E^* when $r > \mu_1$. Note that the stability of E^* is determined by the sign of $b^*(\alpha)$, which is a continuous function with respect to α. If $\mu_2 < \beta_2 T_0$, then $\lim_{\alpha\to\infty} V^* = 0$ and there exists $\hat{\alpha} > 0$ such that $\mu_1 - rV^{*2}/(c + V^*)^2 > 0$ for $\alpha > \hat{\alpha}$. Hence, $b^*(\alpha) > 0$ and the IPE E^* becomes stable for $\alpha > \hat{\alpha}$.

If $\beta_2 T_0/\mu_2 \le 1 < R_0^0$ and $r \le r_m$, then $\lim_{\alpha\to\alpha_t} V^* = 0$ still holds. Similarly, E^* is stable when α exceeds a critical value which is less than α_t. If $\beta_2 T_0/\mu_2 \le 1 < R_0^0$ and $r > r_m$ or $R_0^0 \le 1$ and $r > r_n$, then $b_0 = 0$ at $\alpha = \alpha_s$, which implies $\mu_1 - rV^{*2}/(c+V^*)^2 = s/T^*$, thus $b_1 > 0$ is satisfied. Together with the positivity of b_2, then $b^*(\alpha) > 0$ for $\alpha \in (\alpha_s - \varepsilon, \alpha_s)$ with a small $\varepsilon > 0$. Therefore, E^* is stable before it vanishes.

The aforementioned discussions suggest that E^* becomes stable when α crosses a critical value. This implies that Hopf bifurcation if appears for system (1.1) can only exist in a bounded interval of α. Denote the maximum value of α ensuring the existence of E^* by α_m. If $\inf_{\alpha\in(0,\alpha_m)} b^*(\alpha) > 0$, then E^* is stable whenever it exists. Otherwise, by the continuity of $b^*(\alpha)$, we assume

(**H$_3$**) $\inf_{\alpha\in(0,\alpha_m)} b^*(\alpha) < 0$, $b^*(0) > 0$, $b^*(\alpha)$ has exactly two simple positive zeros $\alpha_1 < \alpha_2$.

This assumption implies that $b^*(\alpha) < 0$ for $\alpha \in (\alpha_1, \alpha_2) := I_1$ and $b^*(\alpha) > 0$ for $\alpha \in (0, \alpha_1) \cup (\alpha_2, \alpha_m) := I_2$. Hence, the IPE E^* is stable if $\alpha \in I_2$ and becomes unstable if $\alpha \in I_1$. The Hopf bifurcation happens at $\alpha = \alpha_i$ $(i = 1, 2)$. In addition, by the geometric property of $b^*(\alpha)$, we have

$$\left.\frac{db^*(\alpha)}{d\alpha}\right|_{\alpha=\alpha_1} < 0,\quad \left.\frac{db^*(\alpha)}{d\alpha}\right|_{\alpha=\alpha_2} > 0.$$

If a Hopf bifurcation exists, then the characteristic equation (3.4) admits a pair of purely imaginary eigenvalues $\pm i\omega_0$ at the bifurcation value. Hence, the eigenvalues of (3.4) are $\lambda_1 = -b_2$, $\lambda_2 = i\sqrt{b_0/b_2}$ and $\lambda_3 = -i\sqrt{b_0/b_2}$, respectively. The period of the periodic solution near the bifurcation value is $P = 2\pi\sqrt{b_2/b_0}$. To summarize, we have the following results.

Theorem 4.4. *Let R_0^0, α_t, α_s, r_m, and r_n be defined in (4.2), (4.3), (4.10), (4.9), and (4.11), respectively.*

(i) *Assume $\mu_2 < \beta_2 T_0$. The unique IPE E^* is locally asymptotically stable for $\alpha \in (0, \infty)$ if $\inf_{\alpha\in(0,\infty)} b^*(\alpha) > 0$. Otherwise, E^* is locally asymptotically stable for $\alpha \in (0, \alpha_1) \cup (\alpha_2, \infty)$ and unstable for $\alpha \in (\alpha_1, \alpha_2)$ when (**H$_3$**) holds.*

(ii) *Assume $\beta_2 T_0/\mu_2 \le 1 < R_0^0$ and $r \le r_m$. The unique IPE E^* is locally asymptotically stable for $\alpha \in (0, \alpha_t)$ if $\inf_{\alpha\in(0,\alpha_t)} b^*(\alpha) > 0$. Otherwise, E^* is locally asymptotically stable for $\alpha \in (0, \alpha_1) \cup (\alpha_2, \alpha_t)$ and unstable for $\alpha \in (\alpha_1, \alpha_2)$ when (**H$_3$**) holds.*

(iii) *Assume $\beta_2 T_0/\mu_2 \le 1 < R_0^0$ and $r > r_m$ or $R_0^0 \le 1$ and $r > r_n$. The IPE E_1^* is locally asymptotically stable for $\alpha \in (0, \alpha_s)$ if $\inf_{\alpha\in(0,\alpha_s)} b^*(\alpha) > 0$. Otherwise, E_1^* is locally asymptotically stable for $\alpha \in (0, \alpha_1) \cup (\alpha_2, \alpha_s)$ and unstable for $\alpha \in (\alpha_1, \alpha_2)$ when (**H$_3$**) holds.*

Moreover, a Hopf bifurcation occurs at $\alpha = \alpha_i$ $(i = 1, 2)$ for system (1.1), and the period of the bifurcated periodic solution at $\alpha = \alpha_i$ is $P_i = 2\pi\sqrt{b_2(\alpha_i)/b_0(\alpha_i)}$.

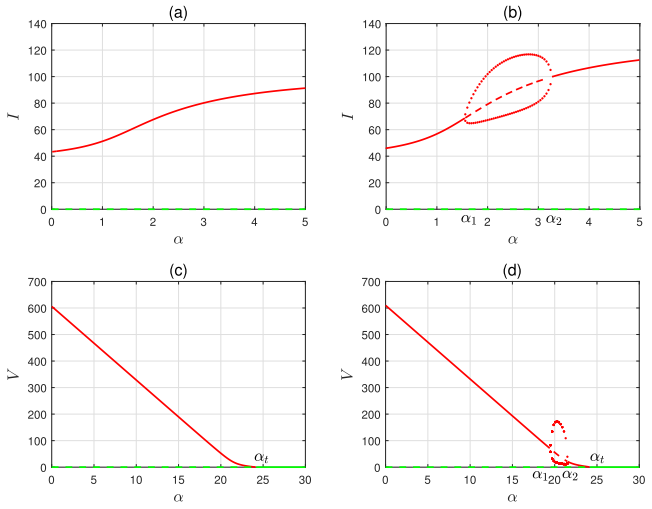


Fig. 2. Bifurcation diagram of infected cells ((a)–(b)) and free viruses ((c)–(d)) with α as the bifurcation parameter. The parameters are: (a) $r = 2$, $\beta_2 = 0.017$; (b) $r = 2.5$, $\beta_2 = 0.017$; (c) $r = 2.3$, $c = 20$, $\beta_1 = 0.15$; (d) $r = 2.9$, $c = 20$, $\beta_1 = 0.15$. The green solid (resp. dashed) line represents the stable (resp. unstable) IFE E_0. α_1 and α_2 are the two Hopf bifurcation values. A transcritical bifurcation occurs at $\alpha = \alpha_t$.

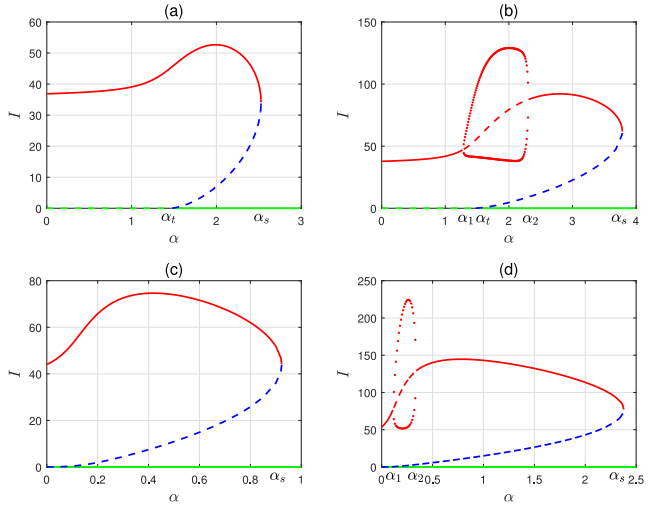


Fig. 3. Bifurcation diagram of infected cells with α as the bifurcation parameter. The parameters are: (a) $r = 0.8$; (b) $r = 0.96$; (c) $r = 0.74$, $\beta_1 = 0.00087$; (d) $r = 0.9$, $\beta_1 = 0.00087$. A saddle–node bifurcation appears at $\alpha = \alpha_s$ and a transcritical bifurcation occurs at $\alpha = \alpha_t$.

Bifurcation simulations are conducted in Figs. 2 and 3 to visualize the theoretical results and show rich viral dynamics. The parameters are selected as $s = 10$, $c = 3$, $\beta_1 = 0.01$, $\beta_2 = 0.002$, $k = 40$, $\mu_1 = 0.6$, $\mu_2 = 0.28$, $\mu_3 = 2.4$ unless otherwise specified. If $\mu_2 < \beta_2 T_0 \approx 0.2833$, then a unique IPE E^* exists and the IFE E_0 is unstable for all $\alpha > 0$, see Fig. 2(a) and (b). If the effect of the viral stimulation is strong, then two Hopf bifurcation values α_1 and α_2 occur. The IPE E^* becomes unstable together with stable periodic solutions for $\alpha \in (\alpha_1, \alpha_2)$, see Fig. 2(b). This conforms to the results shown in case (i) of Theorem 4.4. Similar dynamics illustrating the case (ii) of Theorem 4.4 are formulated in Fig. 2(c) and (d). The value of V^* decreases as α increases, which agrees with the results of Theorem 4.2. We have shown that $\alpha = \alpha_t$ is equivalent to $R_0 = 1$, then E_0 becomes stable if $\alpha > \alpha_t$. Consequently, system (1.1) undergoes a transcritical bifurcation when α passes through the bifurcation value α_t.

Other two conditions presented in case (iii) of Theorem 4.4 are illustrated in Fig. 3(a)–(b) and Fig. 3(c)–(d), respectively. As the loss rate of virus enlarges, the value of I_1^* increases and then decreases, while I_2^* increases consistently. Similarly, Hopf bifurcation occurs for large r, and system (1.1) still has two Hopf bifurcation values α_1 and α_2, see Fig. 3(b) and (d). It is observed from Fig. 3(a)–(b) and Fig. 3(c)–(d) that bistability dynamics exist for $\alpha \in (\alpha_t, \alpha_s)$ and $\alpha \in (0, \alpha_s)$, respectively. Two stable equilibria E_1^* and E_0 or the stable E_0 and a stable limit cycle coexist. Furthermore, E_0 is always stable when $R_0^0 \approx 0.9821 < 1$, see Fig. 3(c) and (d). If bistability phenomenon appears, the long-time behavior of any solution to (1.1) is determined by the initial condition. This suggests us to regulate the populations of cells and viral particles to the basin of attraction of E_0, which corresponds to the extinction of free viruses. On the other hand, if the initial value lies in the basin of attraction of a positive equilibrium or a periodic solution, the viral infection can persist and eventually approach to a positive constant level or a sustained oscillation.

Note that the stable IFE E_0 is the unique equilibrium when α is sufficiently large; namely, $\alpha > \alpha_t$ in Fig. 2(c) and (d), and $\alpha > \alpha_s$ in Fig. 3. This implies that enhancing the impact of viral decay on free viruses can effectively inhibit viral replication and even lead to the eradication of virions under certain conditions. Therefore, it is crucial to investigate and comprehend the virion decay mechanism in order to better control virus infection and transmission. Numerical results also suggest that high proliferation ability of uninfected cells may destabilize the positive equilibrium and induce sustained oscillations. Consequently, it is critical to measure the contribution of viral stimulation to T-cell recruitment in the process of HIV infection, which helps us to better figure out viral kinetics and provide more effective containment strategies.

4.3. Global continuation of Hopf bifurcation

Theorem 4.4 provides sufficient conditions on the existence of periodic solutions bifurcated at the infection persistent equilibrium when the loss rate of virions α passes through the local Hopf bifurcation value. By Lemma 3.1, we assume $R_0 > 1$ to investigate the global continuation of Hopf bifurcation when the condition (i) of Theorem 4.4 and ($\mathbf{H_3}$) are satisfied. Other cases in Theorem 4.4 can be analyzed by using a similar method. Let $u(t) = (T(t), I(t), V(t))^T$, then model (1.1) can be rewritten as

$$u'(t) = F(u(t), \alpha, P), \quad (t, \alpha, P) \in \mathbb{R}_+ \times I_1 \times \mathbb{R}_+, \tag{4.12}$$

where $u(t) \in \mathbb{R}_+^3$, $I_1 = (\alpha_1, \alpha_2)$ and

$$F(u, \alpha, P) = \begin{pmatrix} s - \mu_1 u_1 + \dfrac{r u_1 u_3}{c + u_3} - \beta_1 u_1 u_3 - \beta_2 u_1 u_2 \\ \beta_1 u_1 u_3 + \beta_2 u_1 u_2 - \mu_2 u_2 \\ k u_2 - \mu_3 u_3 - \alpha u_1 u_3 \end{pmatrix}$$

for $u = (u_1, u_2, u_3)^T$. Clearly, F is twice continuously differentiable, thus the assumption (**A1**) in [44] is satisfied. Denote the set of stationary solutions of (4.12) by

$$\mathbf{N}(F) = \{(u, \alpha, P) \in \mathbb{R}_+^3 \times I_1 \times \mathbb{R}_+ : F(u, \alpha, P) = 0\}.$$

If $R_0 > 1$ holds, it then follows from Theorem 4.4 that $\mathbf{N}(F) = \{(E_0, \alpha, P), (E^*, \alpha, P)\}$. For any stationary solution (u, α, P), the characteristic equation of (4.12) is

$$\Delta_{(u,\alpha,P)}(\lambda) = \lambda I - DF(u, \alpha, P),$$

where $DF(u, \alpha, P)$ is the Jacobian matrix of F at the stationary solution. We have shown that 0 is not the eigenvalue of any stationary solution. This suggests that the statement (**A2**) in [44] is satisfied. Furthermore, it can be clearly checked that (**A3**) in [44] also holds.

The results in Theorem 4.4 indicate that the stationary solution (E^*, α_j, P) is an isolated center of (4.12) for $j = 1, 2$, where $P = 2\pi/\omega_j$ and $\omega_j = \sqrt{b_0(\alpha_j)/b_2(\alpha_j)}$. Only one purely imaginary eigenvalue of

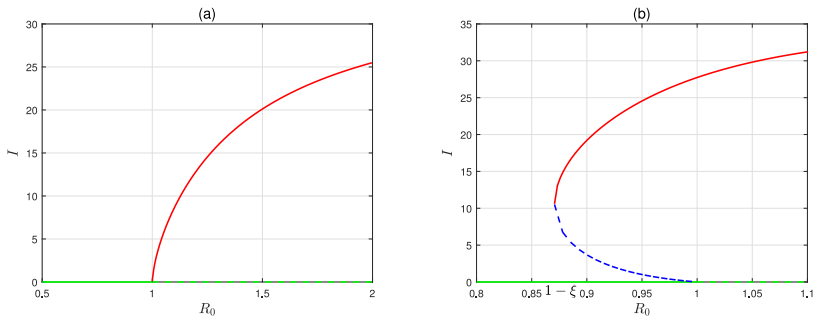


Fig. 4. Bifurcation diagram of infected cells with R_0 as the bifurcation parameter. (a) A forward bifurcation exists at $R_0 = 1$. (b) A saddle–node bifurcation and a backward bifurcation occur at $R_0 \approx 0.8707$ and $R_0 = 1$, respectively.

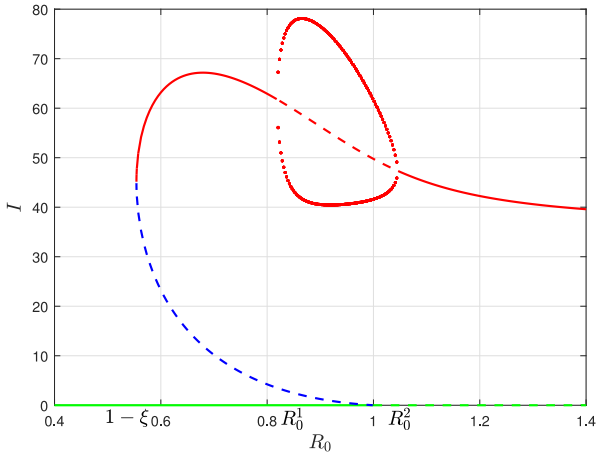


Fig. 5. Bifurcation diagram of infected cells with R_0 as the bifurcation parameter. A saddle–node bifurcation and a backward bifurcation occur at $R_0 \approx 0.5541$ and $R_0 = 1$, respectively. Two Hopf bifurcation values $R_0^1 \approx 0.8192$ and $R_0^2 \approx 1.0449$ exist. The stable IPE becomes unstable together with sustained oscillations for $R_0 \in (R_0^1, R_0^2)$.

the form $im\frac{2\pi}{P}$ exists with $m = 1$. Moreover, the crossing number $\gamma(E^*, \alpha_j, 2\pi/\omega_j)$ follows

$$\gamma(E^*, \alpha_j, 2\pi/\omega_j) = -\text{Sign}\left\{\frac{d\,Re\lambda(\alpha)}{d\alpha}\Big|_{\alpha=\alpha_j}\right\} = \begin{cases} -1, & j = 1, \\ 1, & j = 2, \end{cases} \tag{4.13}$$

which implies that **(A4)** in [44] is satisfied. Then we define a closed subset $\Sigma(F)$ of $\mathbb{R}^3_+ \times I_1 \times \mathbb{R}_+$ by

$$\Sigma(F) = Cl\{(u, \alpha, P) \in \mathbb{R}^3_+ \times I_1 \times \mathbb{R}_+ : \ u \text{ is a nontrivial P-periodic solution of (4.12)}\}.$$

We denote by $\mathbf{C}(E^*, \alpha_j, 2\pi/\omega_j)$ the connected component of $(E^*, \alpha_j, 2\pi/\omega_j)$ in $\Sigma(F)$ for $j = 1, 2$. By Theorem 4.4, $\mathbf{C}(E^*, \alpha_j, 2\pi/\omega_j)$ is a nonempty subset of $\Sigma(F)$. It follows from Theorem 2.1 and Lemma 3.1 that the following results can be directly concluded.

Lemma 4.1. *If $R_0 > 1$ and $r < (\sqrt{\mu_1} + \sqrt{\beta_1 c})^2$, then all nonnegative periodic solutions of system (4.12) are bounded, that is, $\epsilon \le T(t), I(t), V(t) \le M$ for all $t \in \mathbb{R}_+$, where $M = \max\{\overline{T}, \overline{I}, \overline{V}\}$ defined in Theorem 2.1 and $\epsilon > 0$ defined in Lemma 3.1.*

Lemma 4.1 indicates that the projection of $\mathbf{C}(E^*, \alpha_j, 2\pi/\omega_j)$ onto $\mathbb{R}^3_+$ is bounded for $j = 1, 2$. Later numerical simulations show that the periods of the bifurcated periodic solutions are all bounded. Without loss of generality, we assume that the periods of all bifurcated periodic solutions are bounded for $\alpha \in I_1$. Hence, the projection of $\mathbf{C}(E^*, \alpha_j, 2\pi/\omega_j)$ onto P is bounded. To summarize, the global continuation of Hopf bifurcation can be described as follows.

Theorem 4.5. *Assume that $\mu_2 < \beta_2 T_0$, $r < (\sqrt{\mu_1} + \sqrt{\beta_1 c})^2$, $(\mathbf{H}_3)$ is satisfied and the periods of all periodic solutions are bounded for $\alpha \in I_1$, then the two global Hopf branches $\mathbf{C}(E^*, \alpha_j, 2\pi/\omega_j)$ $(j = 1, 2)$ are bounded and collide together.*

Proof. We have shown that $\mathbf{C}(E^*, \alpha_j, 2\pi/\omega_j)$ $(j = 1, 2)$ is bounded in $\mathbb{R}^3_+ \times I_1 \times \mathbb{R}_+$ based on the assumptions. By Lemma 4.1, the periodic solutions are all bounded away from zero. This implies that there is no need to consider the boundary equilibrium IFE. Define $\mathbf{N}_1(F) = \{(E^*, \alpha, P),\ (\alpha, P) \in I_1 \times \mathbb{R}_+\}$. It then follows from (4.13) and the global Hopf bifurcation theorem [44, Theorem 3.3] that $\mathcal{N} := \mathbf{C}(E^*, \alpha_j, 2\pi/\omega_j) \cap \mathbf{N}_1(F)$ is finite and

$$\sum_{(u,\alpha,P)\in\mathcal{N}} \gamma(E^*, \alpha_j, 2\pi/\omega_j) = 0.$$

Therefore, by (4.13), the two global Hopf branches $\mathbf{C}(E^*, \alpha_1, 2\pi/\omega_1)$ and $\mathbf{C}(E^*, \alpha_2, 2\pi/\omega_2)$ coincide with each other and connect a pair of Hopf bifurcation values α_1 and α_2. □

5. Numerical simulations

In this section, we carry out some numerical simulations to reveal rich bifurcation dynamics of system (1.1). We have shown that the basic reproduction number R_0 is the threshold to determine the existence and stability of equilibria. Then we choose R_0 as the bifurcation parameter to visualize such dynamics, see Figs. 4 and 5. It is observed from Fig. 4(a) that a stable IPE E^* appears and the IFE E_0 becomes unstable when $R_0 > 1$, which is in accord with the case (i) of Lemma 2.1 and Theorem 3.1. Hence, a forward bifurcation happens as R_0 passes through the critical value $R_0 = 1$.

It is observed from Fig. 4(b) that a saddle–node bifurcation and a backward bifurcation occur at $R_0 = 1 - \xi \approx 0.8707$ and $R_0 = 1$, respectively. This dynamics exactly confirms to the results shown in case (ii) of Lemma 2.1 and Theorem 3.3. Moreover, bistability dynamics of (1.1) appears where E_1^* and E_0 are both locally asymptotically stable for $R_0 \in (0.8707, 1)$. Note that sufficiently large R_0 can lead to a unique stable IPE existing, and controlling the value of R_0 to be less than 1 is a general effective strategy to suppress the viral dissemination and elimination. However, if there exists a backward bifurcation, then it is indispensable to reduce R_0 to be less than a lower value $1 - \xi$.

When we select a larger value of the proliferation rate r, then similarly to the dynamics shown in Figs. 2 and 3, the stability switches of the IPE and Hopf bifurcation appear with R_0 increasing, see Fig. 5. There still exist two Hopf bifurcation values R_0^1 and R_0^2. We can observe that E_0 is the unique equilibrium which is stable if $R_0 < 1 - \xi$; E_0 and E_1^* are both locally asymptotically stable if $R_0 \in (1 - \xi, R_0^1)$; the stable E_0 and a stable limit cycle coexist if $R_0 \in (R_0^1, 1)$; the limit cycle is the unique attractor of system (1.1) if $R_0 \in (1, R_0^2)$; and E^* is globally

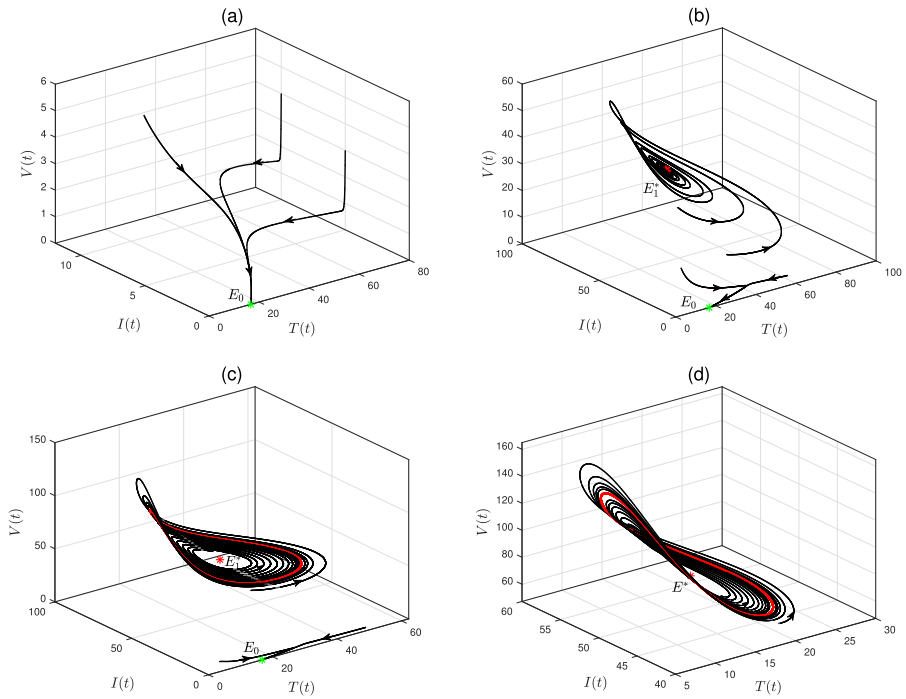


Fig. 6. Illustration of the phase orbits in Fig. 5. The red (resp. green) asterisk denotes the IPE (resp. the IFE). The red curve stands the stable limit cycle. Here the basic reproduction numbers are (a) $R_0 = 0.5$; (b) $R_0 = 0.75$; (c) $R_0 = 0.85$; (d) $R_0 = 1.02$.

asymptotically stable if $R_0 > R_0^2$. The corresponding phase orbits are depicted in Fig. 6, respectively. Furthermore, the basin of attraction of two limit sets is separated by the stable manifolds of the saddle point E_2^* in Fig. 6(b) and (c).

6. Conclusion and discussion

In this paper, we proposed a within-host HIV infection model that incorporates two transmission modes: virus-to-cell and cell-to-cell transmissions. Additionally, we accounted for the stimulation of free viruses on the proliferation of uninfected target cells and loss term of virions due to encountering with target cells. We established the nonnegativity and boundedness of the solutions, and identified the existence of a unique infection free equilibrium (IFE) E_0 and, potentially, up to two infection persistent equilibria (IPE) E_1^* and E_2^*.

Utilizing suitable Lyapunov function and employing the geometric approach introduced by Li and Muldowney [38,39], we demonstrated the global asymptotic stability of E_0 and E^* (or E_1^*), respectively. Additionally, we also verified that another IPE E_2^* is unstable whenever it exits. Furthermore, we established the basic reproduction number R_0 as the threshold for determining the existence and stability of equilibria. The expression of R_0 comprises two components, representing the contributions of virus-to-cell and cell-to-cell infection modes to newly infected cells, respectively. This underscores the significance of both viral transmission routes in investigating the HIV mechanism. Note from (2.4) that R_0 is independent of the parameters r and c; that is, the proliferation of healthy target cells stimulated by virions does not affect the value of the basic reproduction number. However, our results revealed that these two parameters significantly affect the dynamics of (1.1) and shall not be neglected.

The previous study [34] relied on the condition $r < \mu_1$ to establish the global stability of their proposed model, focusing solely on the virus-to-cell infection route. In our research, we broaden the scope by examining both viral infection modes and investigating stability dynamics without restrictions on the relationship between r and μ_1. This expanded analysis has revealed novel dynamics, including stability switches of the positive equilibrium, sustained oscillations, and bistability when $r > \mu_1$ holds true. To explore Hopf bifurcation, we selected the proliferation rate of healthy target cells r and the loss rate of virions α as the bifurcation parameters for theoretical analyses and numerical simulations, respectively. Regarding the infected cell population and free viruses, we observed that their sizes both increase with the proliferation rate increasing. Meanwhile, the variation of infected cells is uncertain and viral load decreases as the loss rate of virions increases. We also examined local Hopf bifurcation and its global continuation with α as the bifurcation parameter. Notably, we demonstrated that a sufficiently large value of α can result in either the nonexistence of the positive equilibrium alongside a unique stable infection free equilibrium, or the existence of a unique infected persistent equilibrium which is globally asymptotically stable. In conclusion, our findings suggest that weakening the proliferation ability of healthy cells or enhancing the loss intensity of free viruses effectively suppresses HIV recruitment and transmission. These insights contribute significantly to our understanding of HIV dynamics and may inform strategies for combating the virus.

For further exploration, we selected the basic reproduction number as the bifurcation parameter and conducted numerical simulations to validate our theoretical findings and visualize a range of bifurcation dynamics, including forward, backward, and saddle–node bifurcations. In contrast to previous models [24,26,34], we have omitted the impacts of antiretroviral therapy in our model, as this term does not influence the stability outcomes. Consequently, we have simplified and enhanced earlier methodologies to construct the proposed model. From a biological perspective, viral recruitment and infection processes typically do not occur instantaneously, and time delay plays a significant role in understanding the mechanisms of HIV. Inspired by this notion, we plan to incorporate time delays into our model in future research to investigate their effects on viral dynamics.

CRediT authorship contribution statement

Jiawei Deng: Writing – original draft, Formal analysis. **Hongying Shu:** Writing – review & editing, Writing – original draft, Supervision, Methodology, Investigation, Funding acquisition, Formal analysis, Conceptualization. **Lin Wang:** Writing – review & editing, Supervision. **Xingfu Zou:** Writing – review & editing, Supervision.

Declaration of competing interest

The authors declare that they have no known competing financial interests or personal relationships that could have appeared to influence the work reported in this paper.

Data availability

No data was used for the research described in this paper.

Acknowledgments

H. Shu is partially supported by the National Natural Science Foundation of China (No. 12371495), the Fundamental Research Funds for the Central Universities, China (No. GK202201002, No. GK202402004) and the Natural Science Basic Research Program of Shaanxi (No. 2023-JC-JQ-03). J. Deng is supported by the China Scholarship Council (No. 202206870022). L. Wang is partially supported by the Natural Sciences and Engineering Research Council of Canada (No. RGPIN-2020-04143). X. Zou is partially supported by the Natural Sciences and Engineering Research Council of Canada (No. RGPIN-2022-04744).

References

[1] World health organization, HIV and AIDS: Key facts, 2023, https://www.who.int/news-room/fact-sheets/detail/hiv-aids. (Accessed 20 December 2023).
[2] D.S. Dimitrov, R.L. Willey, H. Sato, L.J. Chang, R. Blumenthal, M.A. Martin, Quantitation of human immunodeficiency virus type 1 infection kinetics, J. Virol. 67 (4) (1993) 2182–2190, http://dx.doi.org/10.1128/jvi.67.4.2182-2190.1993.
[3] S. Gummuluru, C.M. Kinsey, M. Emerman, An in vitro rapid-turnover assay for human immunodeficiency virus type 1 replication selects for cell-to-cell spread of virus, J. Virol. 74 (23) (2000) 10882–10891, http://dx.doi.org/10.1128/jvi.74.23.10882-10891.2000.
[4] D.D. Richman, D.M. Margolis, M. Delaney, W.C. Greene, D. Hazuda, R.J. Pomerantz, The challenge of finding a cure for HIV infection, Science 323 (2009) 1304–1307, http://dx.doi.org/10.1126/science.1165706.
[5] K.M. Merino, C. Allers, E.S. Didier, M.J. Kuroda, Role of monocyte/macrophages during HIV/SIV infection in adult and pediatric acquired immune deficiency syndrome, Front. Immunol. 8 (2017) 1693, http://dx.doi.org/10.3389/fimmu.2017.01693.
[6] A.S. Perelson, P.W. Nelson, Mathematical analysis of HIV-1 dynamics in vivo, SIAM Rev. 41 (1) (1999) 3–44, http://dx.doi.org/10.1137/S0036144598335107.
[7] M.A. Nowak, C.R.M. Bangham, Population dynamics of immune responses to persistent viruses, Science 272 (5258) (1996) 74–79, http://dx.doi.org/10.1126/science.272.5258.74.
[8] P.W. Nelson, A.S. Perelson, Mathematical analysis of delay differential equation models of HIV-1 infection, Math. Biosci. 179 (1) (2002) 73–94, http://dx.doi.org/10.1016/S0025-5564(02)00099-8.
[9] L. Wang, M.Y. Li, Mathematical analysis of the global dynamics of a model for HIV infection of $CD4^+$ t cells, Math. Biosci. 200 (1) (2006) 44–57, http://dx.doi.org/10.1016/j.mbs.2005.12.026.
[10] M. Shen, Y. Xiao, L. Rong, L.A. Meyers, Conflict and accord of optimal treatment strategies for HIV infection within and between hosts, Math. Biosci. 309 (2019) 107–117, http://dx.doi.org/10.1016/j.mbs.2019.01.007.
[11] T. Guo, Z. Qiu, M. Shen, L. Rong, Dynamics of a new HIV model with the activation status of infected cells, J. Math. Biol. 82 (2021) 51, http://dx.doi.org/10.1007/s00285-021-01604-3.
[12] R.V. Culshaw, S. Ruan, A delay-differential equation model of HIV infection of $CD4^+$ T-cells, Math. Biosci. 165 (1) (2000) 27–39, http://dx.doi.org/10.1016/S0025-5564(00)00006-7.
[13] L. Rong, A.S. Perelson, Modeling HIV persistence, the latent reservoir, and viral blips, J. Theoret. Biol. 260 (2) (2009) 308–331, http://dx.doi.org/10.1016/j.jtbi.2009.06.011.
[14] M. Tsiang, J.F. Rooney, J.J. Toole, C.S. Gibbs, Biphasic clearance kinetics of hepatitis B virus from patients during adefovir dipivoxil therapy, Hepatology 29 (6) (1999) 1863–1869, http://dx.doi.org/10.1002/hep.510290626.
[15] H. Dahari, A. Lo, R.M. Ribeiro, A.S. Perelson, Modeling hepatitis C virus dynamics: Liver regeneration and critical drug efficacy, J. Theoret. Biol. 247 (2) (2007) 371–381, http://dx.doi.org/10.1016/j.jtbi.2007.03.006.
[16] F. Zhang, J. Li, C. Zheng, L. Wang, Dynamics of an HBV/HCV infection model with intracellular delay and cell proliferation, Commun. Nonlinear Sci. Numer. Simul. 42 (2017) 464–476, http://dx.doi.org/10.1016/j.cnsns.2016.06.009.
[17] Q. Sattentau, Avoiding the void: cell-to-cell spread of human viruses, Nat. Rev. Microbiol. 6 (11) (2008) 815–826, http://dx.doi.org/10.1038/nrmicro1972.
[18] A. Sigal, J.T. Kim, A.B. Balazs, E. Dekel, A. Mayo, R. Milo, D. Baltimore, Cell-to-cell spread of HIV permits ongoing replication despite antiretroviral therapy, Nature 477 (2011) 95–98, http://dx.doi.org/10.1038/nature10347.
[19] N.L.K. Galloway, G. Doitsh, K.M. Monroe, Z. Yang, I. Muñoz-Arias, D.N. Levy, W.C. Greene, Cell-to-cell transmission of HIV-1 is required to trigger pyroptotic death of lymphoid-tissue-derived CD4 T cells, Cell Rep. 12 (10) (2015) 1555–1563, http://dx.doi.org/10.1016/j.celrep.2015.08.011.
[20] N.M. Dixit, A.S. Perelson, Multiplicity of human immunodeficiency virus infections in lymphoid tissue, J. Virol. 78 (16) (2004) 8942–8945, http://dx.doi.org/10.1128/jvi.78.16.8942-8945.2004.
[21] N.L. Komarova, D. Anghelina, I. Voznesensky, B. Trinité, D.N. Levy, D. Wodarz, Relative contribution of free-virus and synaptic transmission to the spread of HIV-1 through target-cell populations, Biol. Lett. 9 (1) (2013) 20121049, http://dx.doi.org/10.1098/rsbl.2012.1049.
[22] X. Lai, X. Zou, Modeling cell-to-cell spread of HIV-1 with logistic target cell growth, J. Math. Anal. Appl. 426 (1) (2015) 563–584, http://dx.doi.org/10.1016/j.jmaa.2014.10.086.
[23] H. Shu, Y. Chen, L. Wang, Impacts of the cell-free and cell-to-cell infection modes on viral dynamics, J. Dynam. Differential Equations 30 (2018) 1817–1836, http://dx.doi.org/10.1007/s10884-017-9622-2.
[24] P. De Leenheer, H.L. Smith, Virus dynamics: a global analysis, SIAM J. Appl. Math. 63 (4) (2003) 1313–1327, http://dx.doi.org/10.1137/S0036139902406905.
[25] J.E. Pearson, P. Krapivsky, A.S. Perelson, Stochastic theory of early viral infection: continuous versus burst production of virions, PLoS Comput. Biol. 7 (2) (2011) e1001058, http://dx.doi.org/10.1371/journal.pcbi.1001058.
[26] Y. Wang, Y. Zhou, F. Brauer, J.M. Heffernan, Viral dynamics model with CTL immune response incorporating antiretroviral therapy, J. Math. Biol. 67 (2013) 901–934, http://dx.doi.org/10.1007/s00285-012-0580-3.
[27] J.M. Brenchley, D.A. Price, T.W. Schacker, T.E. Asher, G. Silvestri, S. Rao, Z. Kazzaz, E. Bornstein, O. Lambotte, D. Altmann, B.R. Blazar, B. Rodriguez, L. Teixeira-Johnson, A. Landay, J.N. Martin, F.M. Hecht, L.J. Picker, M.M. Lederman, S.G. Deeks, D.C. Douek, Microbial translocation is a cause of systemic immune activation in chronic HIV infection, Nature Med. 12 (12) (2006) 1365–1371, http://dx.doi.org/10.1038/nm1511.
[28] E.A. Hernandez-Vargas, R.H. Middleton, Modeling the three stages in HIV infection, J. Theoret. Biol. 320 (2013) 33–40, http://dx.doi.org/10.1016/j.jtbi.2012.11.028.
[29] V. Natarajan, R.A. Lempicki, I. Sereti, Y. Badralmaa, J.W. Adelsberger, J.A. Metcalf, D.A. Prieto, R. Stevens, M.W. Baseler, J.A. Kovacs, H.C. Lane, Increased peripheral expansion of naive CD4+ T cells in vivo after IL-2 treatment of patients with HIV infection, Proc. Natl. Acad. Sci. USA 99 (16) (2002) 10712–10717, http://dx.doi.org/10.1073/pnas.162352399.
[30] I. Sereti, R.M. Dunham, J. Spritzler, E. Aga, M.A. Proschan, K. Medvik, C.A. Battaglia, A.L. Landay, S. Pahwa, M.A. Fischl, D.M. Asmuth, A.R. Tenorio, J.D. Altman, L. Fox, S. Moir, A. Malaspina, M. Morre, R. Buffet, G. Silvestri, M.M. Lederman, IL-7 administration drives T cell-cycle entry and expansion in HIV-1 infection, Blood 113 (25) (2009) 6304–6314, http://dx.doi.org/10.1182/blood-2008-10-186601.
[31] A.S. Perelson, D.E. Kirschner, R. De Boer, Dynamics of HIV infection of $CD4^+$ T cells, Math. Biosci. 114 (1) (1993) 81–125, http://dx.doi.org/10.1016/0025-5564(93)90043-A.
[32] D. Kirschner, Using mathematics to understand HIV immune dynamics, Notices Amer. Math. Soc. 43 (1996) 191–202.
[33] D.E. Kirschner, G.F. Webb, A mathematical model of combined drug therapy of HIV infection, J. Theoretical Med. 1 (1) (1997) 25–34, http://dx.doi.org/10.1080/10273669708833004.
[34] H. Shu, L. Wang, Role of $CD4^+$ T-cell proliferation in HIV infection under antiretroviral therapy, J. Math. Anal. Appl. 394 (2) (2012) 529–544, http://dx.doi.org/10.1016/j.jmaa.2012.05.027.
[35] Y.A. Kuznetsov, Elements of Applied Bifurcation Theory, Springer New York, NY, 2004, http://dx.doi.org/10.1007/978-1-4757-3978-7.
[36] L. Perko, Differential Equations and Dynamical Systems, Springer New York, NY, 2001, http://dx.doi.org/10.1007/978-1-4613-0003-8.
[37] X.-Q. Zhao, Dynamical Systems in Population Biology, second ed., CMS Books in Mathematics, Springer, Cham, 2017, http://dx.doi.org/10.1007/978-3-319-56433-3.
[38] M.Y. Li, J.S. Muldowney, On Bendixson's criterion, J. Differential Equations 106 (1) (1993) 27–39, http://dx.doi.org/10.1006/jdeq.1993.1097.
[39] M.Y. Li, J.S. Muldowney, A geometric approach to global-stability problems, SIAM J. Math. Anal. 27 (4) (1996) 1070–1083, http://dx.doi.org/10.1137/S0036141094266449.
[40] J.S. Muldowney, Compound matrices and ordinary differential equations, Rocky Mountain J. Math. 20 (4) (1990) 857–872, http://dx.doi.org/10.1216/rmjm/1181073047.
[41] W.A. Coppel, Stability and Asymptotic Behavior of Differential Equations, Heath, Boston, 1965.
[42] R.H. Martin, Logarithmic norms and projections applied to linear differential systems, J. Math. Anal. Appl. 45 (2) (1974) 432–454, http://dx.doi.org/10.1016/0022-247X(74)90084-5.
[43] P. Yu, Closed-form conditions of bifurcation points for general differential equations, Int. J. Bifurcation Chaos 15 (4) (2005) 1467–1483, http://dx.doi.org/10.1142/S0218127405012582.
[44] J. Wu, Symmetric functional differential equations and neural networks with memory, Trans. Amer. Math. Soc. 350 (12) (1998) 4799–4838, http://dx.doi.org/10.1090/S0002-9947-98-02083-2.